International Geology Review

ISSN: (Print) (Online) Journal homepage: https://www.tandfonline.com/loi/tigr20

Primary minerals and mantle peridotites in Late Cretaceous ophiolites of Iran: a review

Fatemeh Sepidbar, Seyed Masoud Homam, Mohamed Zaki Khedr, Robert J. Stern & Orhan Karsli

To cite this article: Fatemeh Sepidbar, Seyed Masoud Homam, Mohamed Zaki Khedr, Robert J. Stern & Orhan Karsli (2023): Primary minerals and mantle peridotites in Late Cretaceous ophiolites of Iran: a review, International Geology Review, DOI: 10.1080/00206814.2023.2166603

To link to this article: https://doi.org/10.1080/00206814.2023.2166603

INTERNATIONAL GEOLOGY REVIEW
https://doi.org/10.1080/00206814.2023.2166603

Primary minerals and mantle peridotites in Late Cretaceous ophiolites of Iran: a review

Fatemeh Sepidbar[a], Seyed Masoud Homam[a], Mohamed Zaki Khedr[b], Robert J. Stern[c] and Orhan Karsli[d]

[a]Department of Geology, Faculty of Science, Ferdowsi University of Mashhad, Mashhad, Iran; [b]Department of Geology, Faculty of Science, Kafrelsheikh University, Kafr El- Sheikh, Egy; [c]Geosciences Department, University of Texas at Dallas, Richardson, TX, USA; [d]Department of Geological Engineering, Karadeniz Technical University, Turkey

ABSTRACT

Several Mesozoic ophiolites in Iran formed in response to Late Cretaceous subduction initiation. Here we review the geology, petrography, mineralogy and geochemistry of mantle rocks from the Nain, Neyriz, Khoy, Esfandagheh and Fannuj ophiolites. They are remnants of Neo-Tethys ocean lithosphere formed during subduction initiation and were emplaced onto the southern flank of Eurasia. Most show SSZ-type geochemical affinity. We summarize the composition of mantle sections from these five representatives, which comprise lherzolites and harzburgites with minor dunite lenses and sometimes chromitites. Spinels in lherzolite from all regions are characterized by low chromium number [Cr# = Cr/(Al + Cr)] of 0.09 to 0.56 and plot in the abyssal peridotite field, whereas spinel in harzburgite and dunite-chromitite have Cr# of 0.41 to 0.73 and 0.45 to 0.86, respectively, showing geochemical affinities with forearc peridotites and boninites, respectively. Lherzolites and harzburgites have low rare earth element (REE) contents and experienced around 15% and 25% partial melting, respectively. Ophiolitic peridotites from the Nain (inner Zagros ophiolitic belt), Khoy, and Neyriz (outer Zagros ophiolitic belt) complexes are depleted in light REE and show flat heavy REE patterns. By contrast, peridotites from the Fannuj (Makran ophiolitic zone) and Esfandagheh (outer Zagros ophiolitic belt) complexes are characterized by flatter and U-shaped REE patterns, respectively, similar to those of SSZ peridotites. Based on the compositions of olivine and spinel, we infer that chromitites and their dunite envelopes experienced wider variations in oxygen fugacity (fO_2), equilibrium temperatures, and spinel Cr# values than those of the surrounding lherzolites and harzburgites, suggesting interaction between residual mantle harzburgites and H_2O-rich and highly oxidized SSZ melts. Lherzolites from all regions and harzburgites of Nain, Neyriz and Fannuj are MOR-type peridotites that plot in the overlapping space of MOR peridotites and were generated in an extensional environment. These are forearc peridotites that were in equilibrium with tholeiitic melts generated during early proto-forearc or back-arc spreading during subduction initiation, whereas spinels of dunites and high-Cr chromitites were in equilibrium with boninitic melts.

ARTICLE HISTORY
Received 22 August 2022
Accepted 01 January 2023

KEYWORDS
Subduction initiation; boninite; Supra-subduction zone; ophiolite; Iran

1. Introduction

Ophiolites are slices of oceanic lithosphere that have been obducted onto a continental margin and can be classified as mid-oceanic ridge (MOR) or suprasubduction zone (SSZ) types based on the tectonic setting in which they originally formed (Pearce *et al*. 2000; Shervais 2001). Dilek and Furnes (2011) classified ophiolites into: (1) subduction-related types, comprising supra-subduction zone (SSZ) and volcanic arc environments, and (2) subduction-unrelated types, which form at continental margins, mid-ocean-ridge (MOR) systems, and above mantle plumes. Although there is a great overlap in petrological character between both types, ophiolites generated in a MOR setting are generally characterized by fertile mantle rocks with Al-rich spinels (Cr# = atomic Cr/ (Cr + Al) < 0.6) and a relatively low fO_2 (Dilek and Thy 2009; Arai *et al*. 2011; Khedr *et al*. 2014). In contrast, SSZ-type ophiolites, which contain refractory mantle peridotites, have high-Cr# (>0.6) spinels and reflect higher fO_2 (e.g. Dare *et al*. 2009; Arai *et al*. 2011; Khedr and Arai 2013, 2017). Podiform chromitites only form in small volumes within both highly refractory harzburgites and fertile lherzolites, whereas less refractory harzburgites with intermediate-Cr# (0.4–0.6) spinels are the best host rocks for large chromitite pods (Arai 1997; Arai and Miura 2016; Khedr and Arai 2017). The most recent and widely accepted process for the formation of ophiolitic chromitite is melt–rock reaction.

Neotethyan ophiolites define a ~ 7000-km-long belt across southern Eurasia and can be divided into two

CONTACT Seyed Masoud Homam homam@um.ac.ir Department of Geology, Faculty of Science, Ferdowsi University of Mashhad, Mashhad, Iran
Supplemental data for this article can be accessed online at https://doi.org/10.1080/00206814.2023.2166603

groups: (1) Jurassic ophiolites in the west (e.g. the Dinarides and Ligurian ophiolites of S Europe) with MOR-type geochemical signatures and (2) mostly Cretaceous ophiolites in the east, which typically show SSZ-type geochemical features (Abbate *et al*. 1980). Most Neotethyan ophiolites in Cyprus, Turkey, Iran, Pakistan, Afghanistan, and Oman are Late Cretaceous, but some are older (e.g. ophiolites in Caucasus and Iranian Makran).

Previous studies have documented several Iranian ophiolites (Eslami *et al*. (2018), Shirdashtzadeh *et al*. (2017), Torabi (2001), Ghazi *et al*. (2011), Zaeimnia *et al*. (2017), Monsef *et al*. (2010), Rajabzadeh *et al*. (2013), and Sepidbar *et al*. (2021)). Because Cretaceous ophiolites of Iran are mostly related to subduction initiation on the northern margin of Neo-Tethys adjacent to Eurasia (Moghadam and Stern 2015), their geochemistry contains essential information about magmatism and processes associated with subduction initiation. In this paper, we review and characterize peridotites from five Iran ophiolites based on Cr-spinel and peridotite chemistry and use these to discuss the origin and tectonic settings of these units. We describe the geology, petrography, mineralogy and geochemistry of mantle rocks from the Nain, Neyriz, Khoy, Esfandagheh and Fannuj areas in order to better constrain the spatial variation and the geodynamic evolution of Late Mesozoic ophiolites in Iran.

2. Geological setting

Late Mesozoic ophiolites in Iran are found in five belts: (1) Late Cretaceous Zagros Outer Belt Ophiolites (ZOB), which comprise the Khoy and Kermanshah-Kurdistan ophiolites to the NW and the Neyriz and Esfandagheh ophiolites to the SE; (2) Late Cretaceous Zagros Inner Belt Ophiolites (ZIB) containing the Nain, Dehshir, Shahr-e-Babak and Balvard-Baft, Anarak, Posht-e-Badam and Jandaq, Bayazeh ophiolites along the western to south-western periphery of the Central Iranian block; (3) Late Cretaceous-Early Palaeocene Sabzevar-Torbat e-Heydarieh ophiolites of NE Iran; (4) Early to Late Cretaceous Birjand-Nehbandan-Tchehel-Kureh ophiolites in eastern Iran between the Lut and Afghan blocks, and (5) Late Jurassic-Cretaceous Makran ophiolites of SE Iran including the Kahnuj and Fannuj-Maskutan ophiolites. Chromitites occur in most Iranian ophiolites, including Neyriz, Khoy, Esfandagheh (ZOB), Nain (ZIB), which are Harzburgite Ophiolite Type (HOT) ophiolites. They have not been found in others (e.g. Anarak, Posht-e-Badam and Jandaq, Bayazeh), possibly due to poor study in these areas. The Nain, Khoy, Neyriz, Esfandagheh, and Fannuj ophiolites – the foci of our study – are described in greater detail below.

2.1. Nain ophiolite

The Nain ophiolitic complex is located at the northwest margin of the central Iran micro-continental block (Figure 1) (Arai and Torabi 2010; Pirnia *et al*. 2014, 2018). It trends NNW – SSE and is surrounded by Tertiary sedimentary and volcanic rocks in the west and east, respectively. Although shear zones caused fragmentation and displacement, as well as facilitated alteration of ophiolitic rocks, the sequence outcrops in many places in the field area. Mantle rocks consist of peridotite, pyroxenite lenses, and orthopyroxenite veinlets, whereas the thin crustal sequence consists of gabbro, diabase, dyke swarms and pillow lava overlain by pelagic limestone and radiolarite (Figure 2a and 3a). A crust-mantle transition zone is absent and the boundaries between the rock units are chiefly tectonic.

Nain peridotites are mainly serpentinized harzburgite and dunite, whereas lherzolite is relatively fresh. Despite most contacts being tectonic, sharp contacts can occasionally be found between lherzolite and harzburgite and between harzburgite and dunite. Chromitite lenses occur as elongated bodies surrounded by host dunite and harzburgite. The dunite forms wide aureoles around chromite ore bodies, with a gradual (i.e. increasing modal percent of orthopyroxene) transition to harzburgite (Ghazi *et al*. 2010). The lherzolite contains olivine (70 vol. %), orthopyroxene (20 vol. %), clinopyroxene (>10 vol. %) and Cr-spinel (>1 vol. %) with porphyroclastic textures. Other minerals are sulphides, Cr-chlorite and talc. Clinopyroxene occurs as individual grains and small inclusions in orthopyroxene and shows small kink bands in lherzolite (Ghazi *et al*. 2010). Harzburgites consist of olivine (up to 85 vol. %), orthopyroxene (up to 10 vol. %), clinopyroxene (<5 vol. %), and spinel (~1 vol. %). All peridotite samples show diffuse alteration with development of a serpentine-rich matrix. Secondary fibrous amphibole occurs on pyroxene rims. Dunite is the main host rock of chromitite lenses (Ghazi *et al*. 2011). Cr-spinel in the dunite is subhedral to euhedral and is variably altered to thick ferrous chromite at its rims. Chromitite in the Nain ophiolites occurs as aggregates, patches and lenses that include 10, 15 vol. % and ~40 vol. % Cr-spinel, respectively.

2.2. Khoy ophiolite

The Khoy ophiolite is located along the western margin of the Central Iranian block (Figure 1) and may be divided into three lithostratigraphic units: the Eastern Khoy

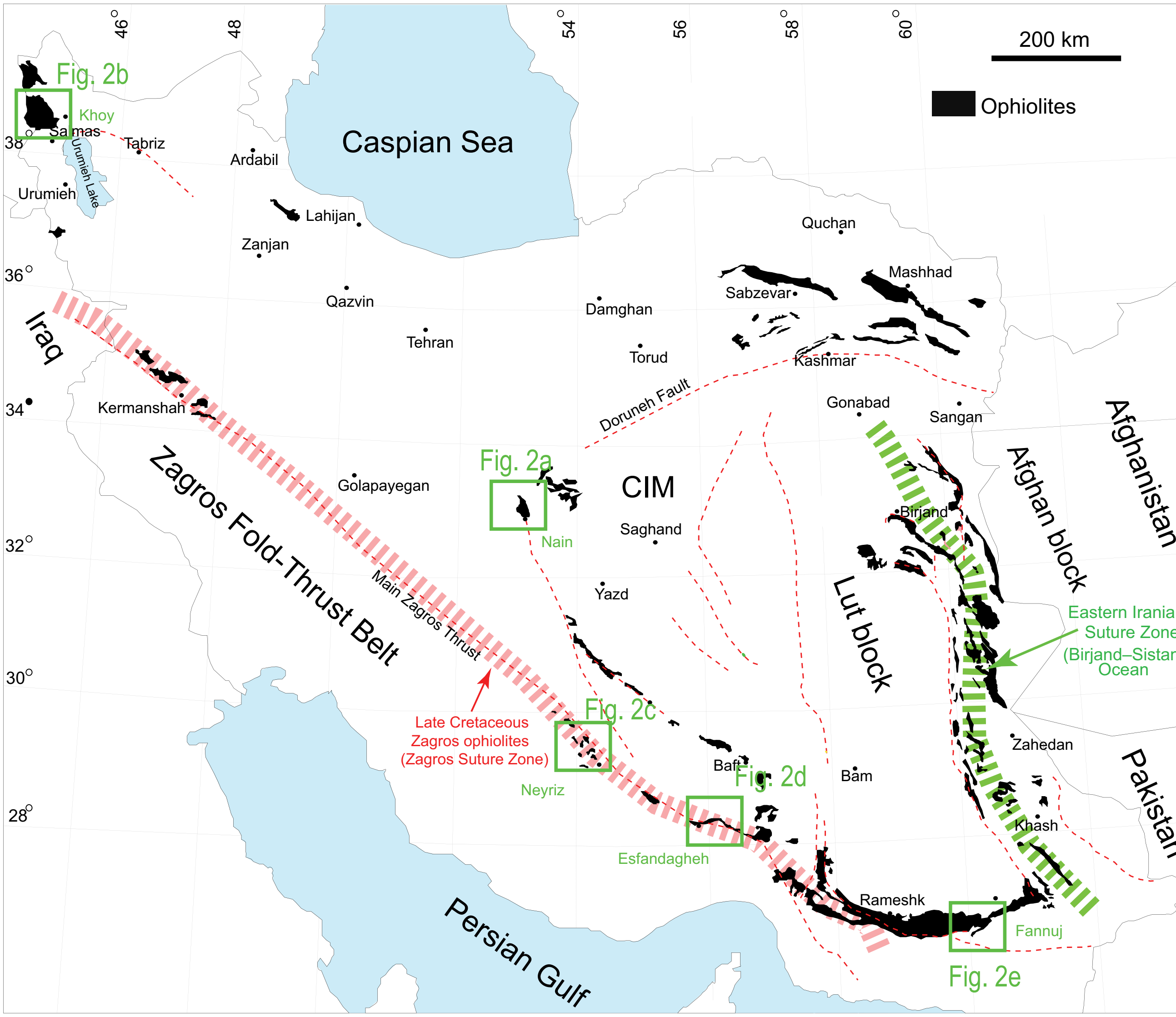

Figure 1. Distribution of Mesozoic ophiolitic complexes within Iran, including the studied Nain, Khoy, Neyriz, Esfandagheh, and Fannuj ophiolites. CIM; central Iranian microcontinent.

Ophiolitic Complex, a central volcanic-turbiditic sedimentary unit, and the Western Khoy Ophiolitic Complex. The NW-trending Eastern Khoy Ophiolitic Complex consists of large tectonic slices of ophiolitic rocks associated with metamorphic rocks. Ophiolitic rocks have been thrusted over the metamorphic rocks in a southwestern direction. Here, we consider the ultramafic tectonites in the middle of the Eastern Khoy Ophiolitic Complex. These ultramafic rocks include lherzolites and clinopyroxene-rich harzburgites, which show obvious high-temperature mantle deformation defined by flattened and stretched orthopyroxene and spinel grains (Monsef *et al*. 2010; Zaeimnia *et al*. 2017). Deformation features such as undulatory extinction and kinking are common. The Khoy area includes serpentinized lherzolites and harzburgites to the east and harzburgites and dunite to the west (Figure 2b and 3b). Lherzolites consist of olivine (ca. 70 vol. %), orthopyroxene (10–20 vol. %), and clinopyroxene (5–10 vol. %) with minor Cr-spinel (<2 vol. %). Clinopyroxenes are diopside that exhibit kinking and twinning. Opaque minerals in the serpentinites are magnetite and Cr-spinel. Some Cr-spinel grains show highly porous ferritchromite rims. The harzburgites are interlayered with numerous dunite and chromitite bodies in western Khoy, similar to those of other ophiolites. They are composed of 70–80 vol. % olivine, 20 vol. % orthopyroxene, 2 vol. % clinopyroxene, and <2 vol. % Cr-spinel. These rocks are highly fractured, which likely allowed fluid ingress to promote intense serpentinization. Cr-spinels are anhedral or amoeboid in shape and occur as disseminated grains. Clinopyroxene occurs as small grains in orthopyroxene. Chromitite occurs as lenticular pods enveloped by dunite within highly serpentinized peridotites in the eastern Khoy ophiolite.

2.3. Neyriz ophiolite

The Neyriz ophiolite is located at the western border of the Zagros Suture Zone, in southern Iran (Figure 1). The mantle section is composed of nearly homogenous harzburgite that is more than 2 km thick, constituting 80% of the ophiolite, and is covered by Late Cretaceous pelagic limestones of the Tarbour Formation. The harzburgite is mixed with numerous dunite and chromitites, similar to those of other ophiolites. Dunite dykes within the clinopyroxene-bearing harzburgite generally range from 20 to 100 cm wide and grade into the host peridotite over a few centimetres to a few tens of centimetres. Minor lherzolite appears as patches within the lower parts of the homogenous harzburgite and lack any obvious relation with host rock. The crustal section includes a thick, massive, and serpentinized dunite that occurs directly at the mantle–crust transition zone and grades progressively into wehrlite. Gabbros is rare in the ophiolite (Rajabzadeh *et al*. 2013) (Figure 2c and 3c). The peridotites are locally cut by dibasic (up to 10 m thick), and orthopyroxenitic (up to 3 m thick) dykes, which are concordant with the foliation of the host ultramafic tectonite.

Ultramafic rocks at the mantle–crust transition zone occur as dismembered fragments at the top of ophiolite pile and consist of dunite, orthopyroxenite, wehrlite, and minor uneconomic disseminated chromitite (Rajabzadeh *et al*. 2013). The residual lherzolite contains 60–65 vol. % olivine, 25–30 vol. % orthopyroxene, 5–7 vol. % clinopyroxene, and 1–3 vol. % Cr-spinel. The main textures of this rock are mosaic and porphyroclastic. Clinopyroxene appears as banded exsolution lamellae and small inclusions in orthopyroxene and as small crystals among olivine and orthopyroxene. Some orthopyroxenes and clinopyroxenes show kink structure. Both olivine and orthopyroxene in the lherzolites experienced deformation, as shown by deformed lamellae along slip planes, kink banding and wavy extinction. Harzburgite is the most abundant rock type and is composed of 70–80 vol. % olivine, 15–25 vol. % orthopyroxene, 1–2 vol. % clinopyroxene, and <2 vol. % Cr-spinel. It exhibits widespread serpentinization, mainly developed along fractures. Amoeboid Cr-spinels occur as disseminated irregular-shaped grains. Clinopyroxene is found as individual discrete grains. All dunites in the Neyriz ophiolite have the same mineral assemblages, comprising mainly olivine (94–97 vol. %) with minor orthopyroxene (2–4 vol. %) and Cr-spinel (1–2 vol. %). Massive chromitites are composed of coarse-grained Cr-spinel (up to 2 cm), with serpentinized olivine and chlorite as matrix silicates minerals. Massive chromitites are composed of coarse-grained chromian spinel crystals (up to 2 cm), with serpentinized olivine and chlorite as gangue minerals (Figure 2g). In contrast, disseminated ores contain smaller (0.2–1 cm) rectangular grains in which olivine and serpentine minerals are the principal interstitial minerals. The effects of tectonic activity and obduction are recorded as cohesive cataclasite and pull-apart structures in some chromitites. Chromitite bodies are characterized by varying shapes and mass (Rajabzadeh *et al*. 2013). In these, Cr-spinel grains constitute aggregates of 1–3 cm nodules within an olivine-rich matrix. Banded chromitites are formed by alternating chromian spinel-rich (mean 1 cm thick) and serpentine-rich bands (up to 5 cm thick) and exhibit pull-apart and cataclastic fabrics (Figure 2i). Most chromite grains in the studied chromitites are fresh, but in some highly serpentinized samples, chromite may exhibit rims characterized by higher reflectance under ore microscope corresponding to secondary ferrian chromite.

2.4. Esfandagheh ophiolite

The Esfandagheh ultramafic massif is part of a series of homogenous peridotite bodies that were emplaced in the ophiolite mélange belt of the Esfandagheh region in southern Kerman province, which hosts several chromitite deposits. This belt is located at the southeastern edge of the main Zagros thrust (Figure 1) and is part of the ZOB (Sepidbar *et al*. 2021; Figure 1). According to McCall (1985), this area is part of the southern margin of the Sanandaj-Sirjan–Bajgan-Durkan (SS-BD) sliver (Figure 2d), separate from Neyriz ophiolites. In contrast, Shahabpour (2005) suggests that these ophiolite mélanges are parts of the Neyriz ophiolite belt along the southeastern edge of the main Zagros thrust.

The dominant mantle lithology of the Esfandagheh melange is harzburgite (90%), with associated dunite, lherzolite, and pyroxenite (10%) (Figure 2d, 3d). Lherzolites occur as small, reddish-brown outcrops in the northern part of the area. Lherzolite–harzburgite contacts are gradational due to variations in the modal percent of clinopyroxene and orthopyroxene. Lherzolites formed first and contained more than 7 vol % clinopyroxene, but later underwent partial melting to produce harzburgite (Peighambari *et al*. 2011) (Figure 2d) containing 66–88 vol. % olivine, 15–27 vol. % orthopyroxene, 1–5 vol. % clinopyroxene, and 1–3 vol. % spinel. The effects of partial melting can be seen in LREE-depleted and nearly flat patterns from Gd to Lu (see next section). Olivine occurs as irregular porphyroclasts and has sinusoidal grain boundaries. In the harzburgites,

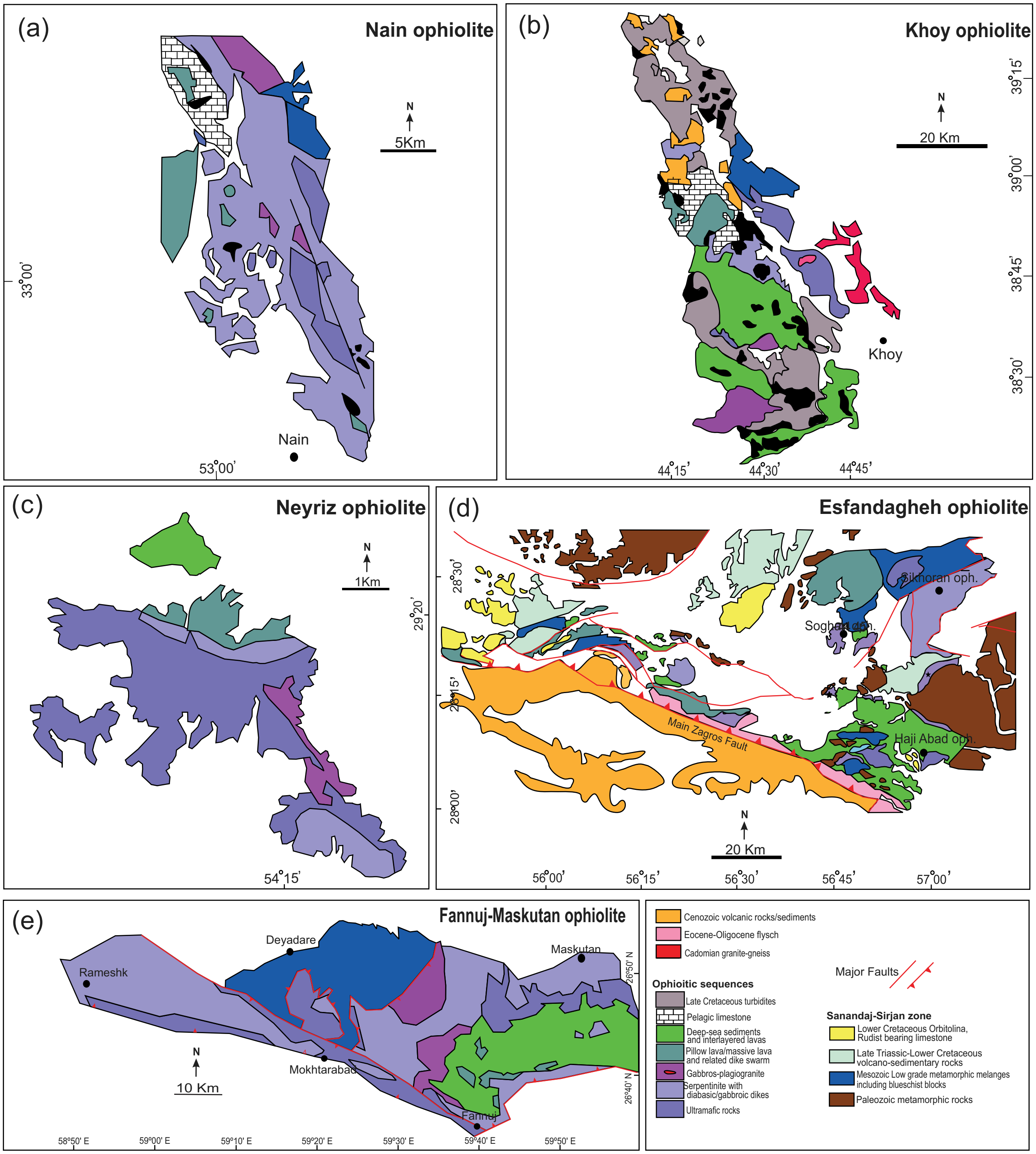

Figure 2. (a) Simplified geological map of the (a) Nain ophiolite (modified after Davoudzadeh, 1972); (b) Khoy ophiolite; (c) Neyriz ophiolite (modified after Monsef *et al*. 2010); (d) Esfandagheh ophiolite (modified after Sepidbar *et al*. 2021); and (e) Fannuj ophiolite (modified after Sepidbar *et al*. 2020).

orthopyroxene dominantly occurs as coarse-grained deformed porphyroclasts (>3 mm in diameter). Such porphyroclasts often show irregular sinusoidal outlines. Minor amounts (up to 5 vol. %) of undeformed orthopyroxene (Opx2) occur as tiny interstitial grains (0.5 to 2 mm in diameter) in the harzburgites. Clinopyroxenes (1–5 vol. %) occur as slightly deformed grains (1–3 mm) along olivine–orthopyroxene grain boundaries. Opx2 crystallized along olivine–olivine grain boundaries or is intermixed with Ol2. Interstitial clinopyroxene (Cpx2) occurs as small grains between orthopyroxene neoblasts or porphyroclasts (Peighambari *et al*. 2011). Petrographically, the lherzolites are similar to harzburgites and consist of

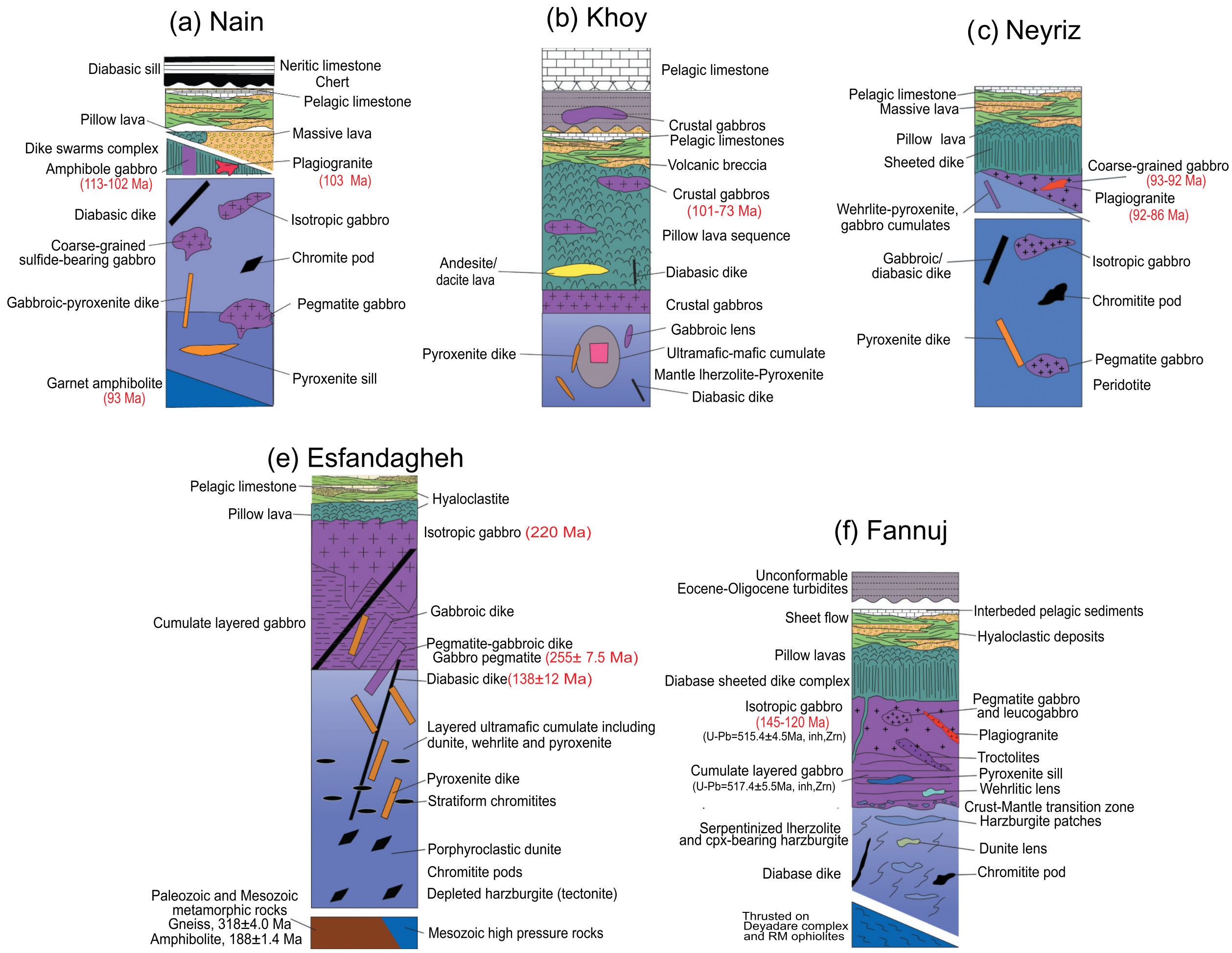

Figure 3. (a) Simplified psuedo-stratigraphic columns of the (a) Nain ophiolite (modified after Davoudzadeh, 1972); (b) Khoy ophiolite; (c) Neyriz ophiolite (modified after Monsef *et al*. 2010); (d) Esfandagheh ophiolite (modified after Sepidbar *et al*. 2021); and (e) Fannuj ophiolite (modified after Sepidbar *et al*. 2020), displaying idealized internal lithologic successions.

different generations of olivine and orthopyroxene but have more clinopyroxene (10–15 vol. %). Clinopyroxenes occur as distinct porphyroclasts with orthopyroxene. They also occur as inclusions in orthopyroxene and as undeformed grains at the boundary of orthopyroxene porphyroclasts. The lherzolites contain brown-reddish Cr-spinels of various size, shape and occurrence. Some Cr-spinels are anhedral to euhedral (up to 3 mm) and occasionally contain olivine inclusions. There are spectacular clinopyroxene +spinel symplectites at the rims of large orthopyroxene porphyroclasts. Dunites consist of coarse-grained olivine (4–5 mm) with 120° triple junctions. Undulatory extinction, deformation lamellae and subgrains occur in many olivines. Minor clinopyroxene (1 vol. %) usually occurs as interstitial grains (1–2 mm) between olivines. Cr-spinels, usually euhedral to subhedral, are typically located at olivine grain boundaries. Spinel occurs either with or without olivine/serpentine inclusions and shows a sieve texture.

2.5. Fannuj ophiolite

The Fannuj ophiolite is located in the central-eastern Makran (Figure 1). It covers an area of ca. 2800 km^2 south of Jaz Murian (see Khalatbari Jafari *et al*. 2016). It is bordered to the west by the Rameshk-Moktharabad ophiolite complex, to the east by the eastern Makran (Kahiri-Espake and Iranshar) ophiolites, and to the south by the Bajgan-Durkan complex and Makran accretionary wedge (e.g. Moghadam and Stern 2015; Khalatbari Jafari *et al*. 2016; Sepidbar *et al*. 2020). The Fannuj-Makran ophiolite (FMO) includes both mantle and crustal sequences (Figure 2e). The mantle sequence is comprised of lherzolites and harzburgites that are mainly exposed in the west (Figure 2e). The primary mantle textures are still preserved, despite their locally tectonized and/or serpentinized character (Khalatbari Jafari *et al*. 2016). The FMO crustal sequence is composed of layered and isotropic gabbros that are overlain by basaltic rocks with associated pelagic sediments. It shows a complete exposure from the basal mantle peridotites to the upper mafic lava sequences with their interlayered pelagic sediments (Figure 2e, 3e).

Primary contacts between mantle rocks, gabbros, and basalts are locally well preserved. Ultramafic rocks representing the upper mantle are overlain by crustal sequences containing lower cumulate layered gabbros that upward gradually transform into isotropic massive gabbros. All FMO peridotites are charged with chromitite and dunite pods. Lower cumulate layered gabbros include pyroxenite and wehrlite lenses, whereas pegmatite-gabbros and plagiogranite pockets are observed in the upper isotropic gabbros.

The main peridotite body is located in the northern FMO complex (Figure 2e), where the dominant rock is lherzolite. This has porphyritic texture with porphyroclasts (1–3 mm in size) and fine-grained matrix (<0.5 mm in size) and is associated with minor clinopyroxene-bearing porphyroclastic (1–3 mm in size) harzburgites (sample Hr1). The harzburgites are highly serpentinized. All peridotite samples display mantle deformation textures, such as foliation and kinked, stretched, and rotated porphyroclasts.

Lherzolites consist mainly of olivine (~70 vol. %), orthopyroxene (10–20 vol. %), clinopyroxene (5–10 vol. %), and spinel (<2 vol. %). Orthopyroxene and spinel locally exhibit symplectitic intergrowths. Harzburgites consist of olivine (up to 85 vol. %), orthopyroxene (up to 10 vol. %), clinopyroxene (<5 vol. %), and spinel (~1 vol. %). All peridotite samples show diffuse alteration, with the development of a serpentine-rich matrix. Secondary fibrous amphibole is locally observed on pyroxene rims.

3. Data sources

We compiled literature data for mineral and whole-rock major and trace-element geochemical compositions for Iranian ophiolites discussed above (Table 3). Nain mantle sequence data (Supplementary Tables S1, S2) are after Eslami *et al*. (2018), Shirdashtzadeh *et al*. (2017), Torabi (2001) and Ghazi *et al*. (2011). Neyriz, Esfandagheh, and Khoy mantle sequence data (Supplementary Table S1, S2) are after Zaeimnia *et al*. (2017), Monsef *et al*. (2010), Rajabzadeh *et al*. (2013), Sepidbar *et al*. (2021), and Peighambari *et al*. (2011); and Fannuj mantle sequence data are after Sepidbar *et al*. (2020).

The fO_2 and crystallization temperatures of the peridotites from Nain, Khoy, Neyriz, Esfandagheh and Fannuj were calculated based on the compositions of coexisting primary olivine and spinel pairs (Ballhaus *et al*. 1990, 1991). Oxygen fugacities of the peridotites were calculated based on these mineral assemblages and are reported as log units relative to the FMQ (fayalite–magnetite–quartz) buffer at 1.5 GPa (Ballhaus *et al*. 1991), where log fO_2 FMQ refers to the deviation from the FMQ conditions (Parkinson and Pearce 1998) (Supplementary Table S3). As Mg and Fe readily exchange between olivine and spinel at high temperatures, we only used core compositions rather than rim compositions in order to only consider primary (unmodified) compositions. This calculated fO_2 is applicable to a variety of mantle-derived rocks. In the discussion below, Y_{Cr}, Y_{Al} and Y_{Fe} are the atomic proportions of Cr, Al and Fe^{+3}, respectively, of the trivalent cation total (Cr + Al + Fe^{+3}).

4. Results

4.1 Mineral chemistry

Compositions of minerals in mantle peridotites are reliable petrogenetic indicators (e.g. Dick and Bullen 1984) that reflect the degree and condition of partial melting alongside the effects of melt-rock interaction. For this reason, detailed chemical characteristics of all available Cr-spinels and olivines within lherzolite, harzburgite, dunite and chromitite of the Nain, Neyriz, Khoy, Esfandagheh and Fannuj-Makutan ophiolites were compiled.

Nain ophiolite

The Cr_2O_3 contents of Cr-spinels from lherzolite, harzburgite and dunites of Nain are 9.1–26.1 wt. %, 33.1–41.9 wt. %, and 35.9–36.9 wt. %, respectively. FeO_T contents range between 11.3 and 23.9 wt. %. The compiled data are characterized by variable MgO (11.7–20.8 wt. %), Al_2O_3 (18.9–58.3 wt. %) and low TiO_2 (<0.5 wt. %) contents. Nain lherzolite contains Cr-spinel with a Cr# [= Cr/(Cr + Al)] of 0.09 to 0.32 (mean at 0.18) and Mg# [= Mg/(Mg + Fe)] of 0.40 to 0.81 (mean at 0.68). Cr-spinel in harzburgite, dunite and chromite has higher Cr# values of 0.41 to 0.54 (mean at 0.47), 0.45 to 0.61 (mean at 0.51), and 0.58 to 0.64 (mean at 0.61), respectively, and lower Mg# values of 0.50 to 0.67 (mean at 0.60), 0.30 to 0.54 (mean at 0.46) and 0.63 to 0.68 (mean at 0.65), respectively.

Cr-spinel in Nain lherzolites plot in the abyssal peridotite field on a Cr–Al–Fe ternary diagram (Figure 4a), close to the Cr–Al dividing side. They lie within the field for MOR peridotite on TiO_2–Cr# and Cr#–Mg# plots of

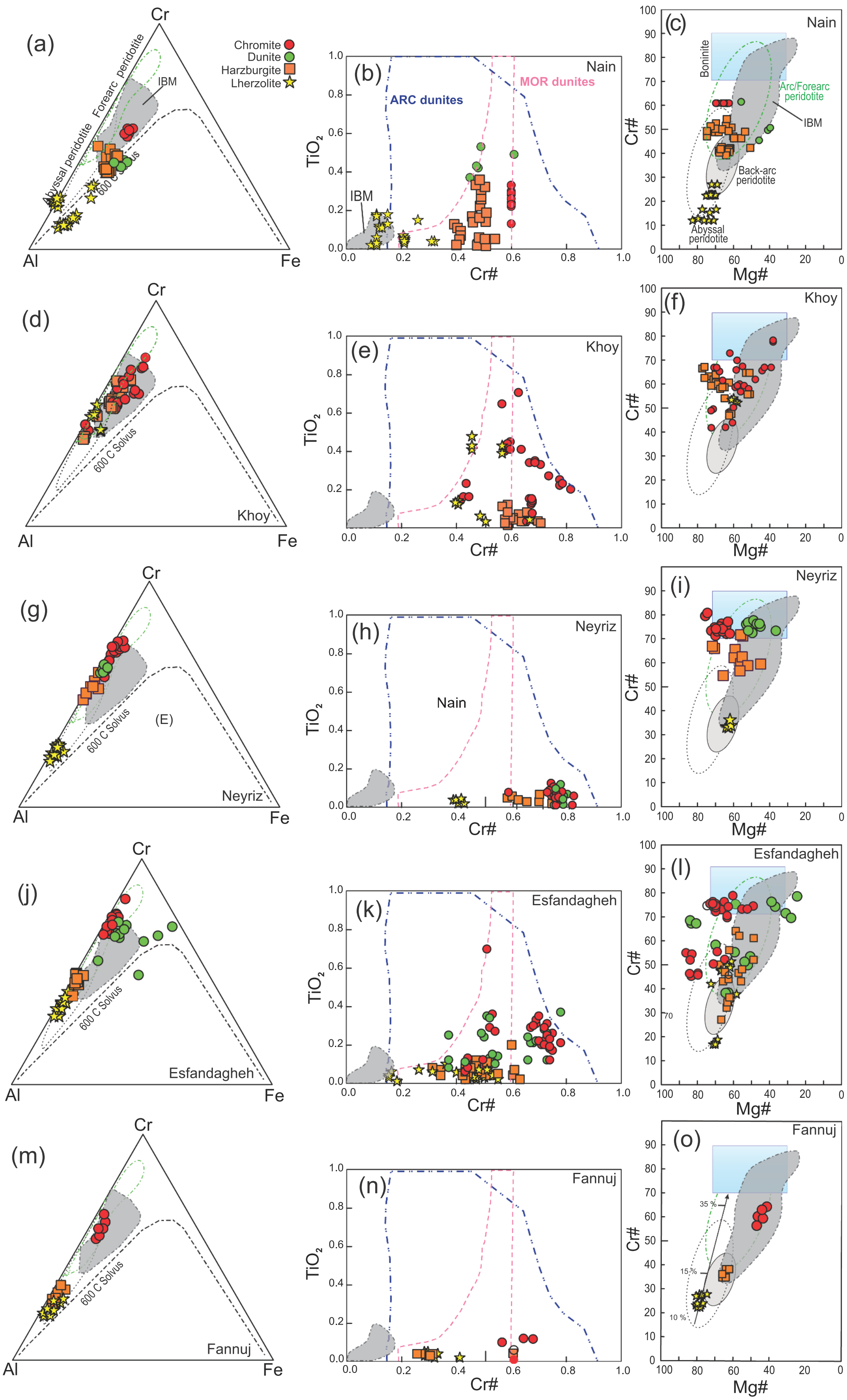

Figure 4. Spinel Al–Cr–Fe^{3+} ternary (a,d,g,j,m), TiO_2-Cr# (b,e,h,k,n) and Cr#-Mg# binary diagrams (c,f,I,l,o) for Nain, Khoy, Neyriz, Esfandagheh and Fannuj ultramafic rocks. The field of abyssal peridotites is after .Arai (1994), Arai *et al.* (2011), and Khedr and Arai (2017), and the field for forearc (SSZ) peridotites is after Ishii *et al.* (1992) and Khedr and Arai (2017)

spinel compositions (Arai *et al*. 2011) (Figure 4b, c). The Cr# of Cr-spinel in harzburgite and dunite overlaps with the ranges for abyssal and forearc peridotites (Arai *et al*. 2011) (Figure 4b, c). Olivine in Nain peridotites is homogenous, with high MgO (48–50 wt. %), very low MnO (0.08–0.15 wt. %), Cr_2O_3 (<0.1 wt. %), NiO of 0.33–0.40 wt. %, and Fo of 89–90 mol. %, and lie within the olivine-mantle array (e.g. Takahashi *et al*. 1987; Moghadam *et al*. 2015) (Figure 5).

Khoy ophiolite

Spinel in Khoy ophiolite peridotites exhibits a wide range of Cr# (0.39–0.81) and Mg# (0.45–0.76) values. The spinel Cr# of lherzolites (0.45–0.53; mean at 0.48) is lower than that of harzburgite (0.39–0.70; mean 0.58) and chromitites (0.41–0.81; mean at 0.62), whereas the spinel Mg# of lherzolites, harzburgite and chromitites ranges 0.46–0.61 (mean at 0.55), 0.48–0.75 (mean at 0.65) and 0.36–0.70 (mean at 0.55), respectively. Al-rich

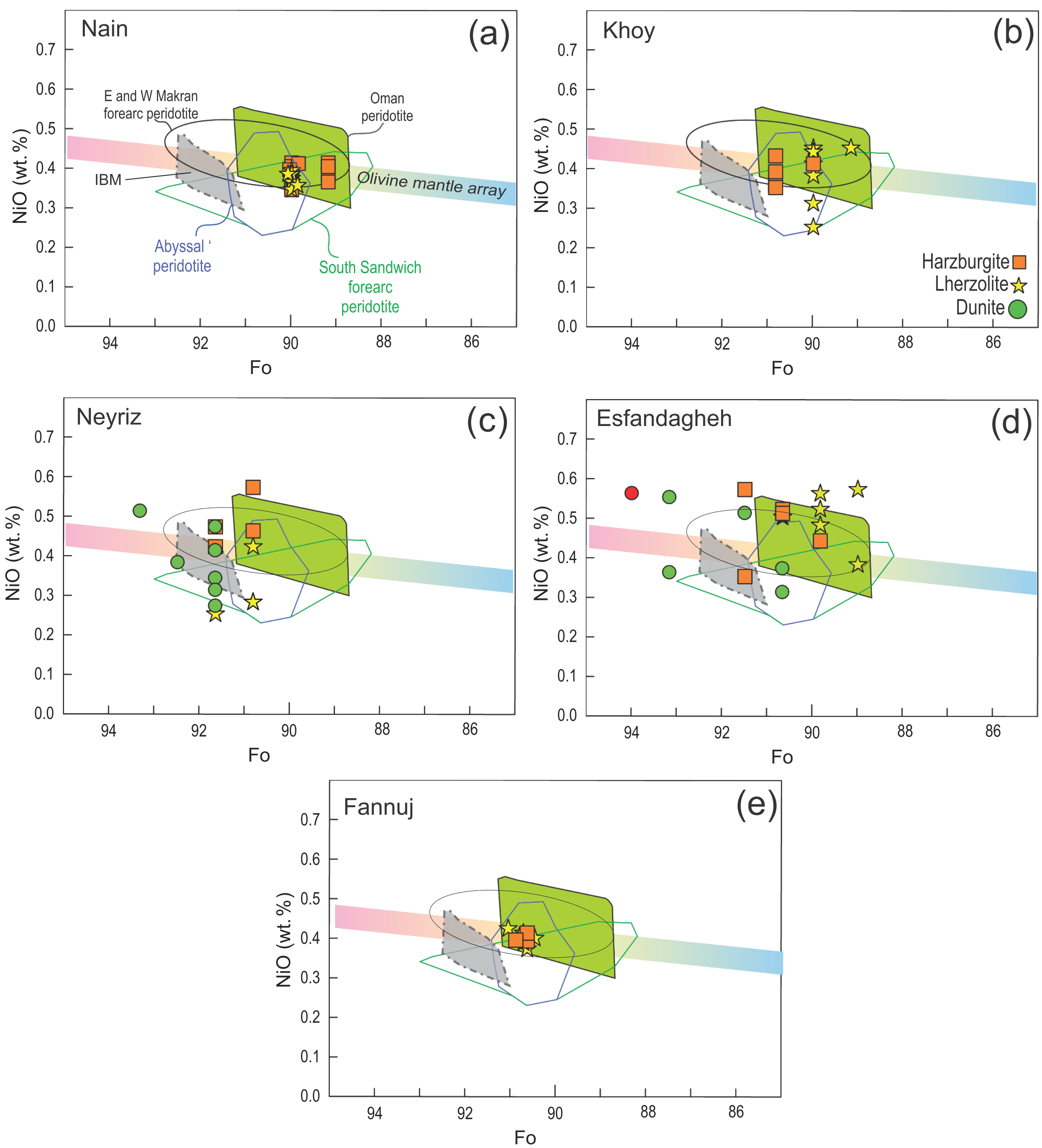

Figure 5. Olivine compositional variations of mantle peridotites from Nain, Khoy, Neyriz, Esfandagheh and Fannuj in the XFo vs NiO diagram (after Pagé et al. 2008).

spinels in the lherzolite show low-to-moderate TiO_2 contents (up to 0.5 wt. %) and high Al_2O_3 contents (26–28 wt. %) (Supplementary Table S1b). Cr-rich spinels in the harzburgite have up to 0.11 wt. % TiO_2 and Al_2O_3 of 8.5–34.9 wt. %, and plot in the overlapping space of abyssal and forearc peridotites (e.g. Arai 1994; Arai *et al*. 2011), respectively.

Olivine in Khoy peridotites is homogenous with high MgO (48–50 wt. %), Mg# (0.89–0.91) and very low MnO (<0.2 wt. %) and Cr_2O_3 up to 0.15 wt. %). NiO is up to 0.40 wt. %. Olivine shows a high forsterite content (Fo: 89–91 mol. %), and lie close to and within the olivine-mantle array field (e.g. Takahashi *et al*. 1987; Moghadam *et al*. 2015) (Figure 4d-f, 5).

Neyriz ophiolite

Data for lherzolites, harzburgites, dunites, and chromitites from the Neyriz ophiolite from Rajabzadeh *et al*. (2013) were used The Cr# of spinel in peridotites and chromitites ranges from 0.37 to 0.46 for lherzolites, 0.58 to 0.73 for harzburgites, 0.74 to 0.79 for dunites, and 0.72 to 0.81 for chromitite. Spinel Mg# ranges from 0.58 to 0.61 (mean at 0.60) for lherzolites, 0.41 to 0.68 for harzburgites (mean at 0.55), 0.32 to 0.49 (mean at 0.44) for dunites, and 0.62 to 0.72 (mean at 0.65) for chromitites (Supplementary Table S1c). Spinels in Neyriz lherzolites plot close to the Cr–Al side on a Cr–Al–Fe ternary diagram, falling in the field of abyssal peridotite, whereas those from harzburgites, dunites and chromitites overlap fields of abyssal and forearc peridotites (Figure 4g) (e.g. Arai 1994; Arai *et al*. 2011; Khedr *et al*. 2014). This agrees with spinel data plotted on TiO_2 vs. Cr# and Cr# vs. Mg# diagrams (Figure 4h, i). Olivine in Neyriz peridotites is also homogenous, with high MgO (48–51 wt. %) and Mg# (0.91–0.95), but low MnO (<0.15 wt. %), Cr_2O_3 (up to 0.2 wt. %), and NiO (0.28 wt. %) contents. Olivine has high forsterite content (Fo: 91–95 mol. %) and plots close the olivine-mantle array field (e.g. Takahashi *et al*. 1987; Moghadam *et al*. 2015) (Figure 5)

Esfandagheh ophiolite

Peridotite and chromitite analyses from Esfandageh ophiolites were compiled from Sepidbar *et al*. (2021) and Peighambari *et al*. (2011). Spinel Cr# ranges 0.16–0.56 for lherzolites, 0.43–0.64 for harzburgites, 0.38–0.76 for dunites and 0.44–0.79 for chromitites. Spinel Mg# is 0.59–0.72 (0.67 on average) for lherzolites, 0.49–0.83 (0.63 on average) for harzburgites, 0.46–0.83 (0.55 on average) for dunites, and 0.51–0.86 (0.71 on average) for chromitite (Supplementary Table S1d). Most Esfandagheh dunite spinels plot in the field of forearc peridotite spinels on the Cr–Al–Fe, TiO_2 vs. Cr# and Cr# vs. Mg# diagrams (Figure 4j-l). However, spinels in host harzburgites and lherzolites overlap fields of abyssal (Figure 4j-l) and forearc peridotites (e.g. Arai 1994; Arai *et al*. 2011; Khedr *et al*. 2014). Esfandagheh peridotite olivines are also characterized by high MgO (48–51 wt. %), Mg# (0.91–0.94) and low MnO (<0.3 wt. %), and Cr_2O_3 (up to 0.23 wt. %). Olivine has a broad range of forsterite contents (Fo: 88–94 mol. %) and plots close to the olivine-mantle array (e.g. Takahashi *et al*. 1987; Moghadam *et al*. 2015) (Figure 5).

Fannuj ophiolite

Cr-spinel analyses of lherzolites, harzburgites and chromitite from Fannuj ophiolite peridotites are after Sepidbar *et al*. (2020). Spinel from lherzolite-harzburgite units has high Al_2O_3 (31.4–43.3 wt. %), Cr_2O_3 (22.3–32.9 wt. %) and FeO_{tot} (17.0–22.5 wt. %) contents, but low TiO_2 (<0.05 wt. %) and MnO (<0.4 wt. %) contents. Spinel Mg# ranges from 0.46 to 0.67 (mean value 0.62) and Cr# lies in the range 0.26 to 0.41 (mean = 0.30) (Supplementary Table S1e). Spinel Mg# and Cr# range from 0.41 to 0.46 (mean 0.43) and 0.61 to 0.68 (mean 0.63), respectively (Supplementary Table S1e). The compositional variation of spinel is shown in Al–Cr–Fe^{3+} ternary and TiO_2–Cr# and Cr#–Mg# binary diagrams (Figure 4m-o), which indicate that this is Al-spinel (Supplementary Table S1e) and mainly plots in the field of abyssal peridotites (Figure 4m). Olivine in Fanuj peridotites is homogenous, with high MgO (50–51 wt. %), Mg# (0.90–0.91), and very low MnO (0.11–0.15 wt. %) and Cr_2O_3 (0.1 wt. %). Its NiO content is 0.38 to 0.42 wt. % and forsterite content (Fo: 90–91 mol. %; forsterite-chrysolite) sits within the olivine-mantle array (e.g. Takahashi *et al*. 1987; Moghadam *et al*. 2015) (Figure 5).

4.2 Whole-rock geochemistry

Whole-rock major and trace-element chemistry (Supplementary Table S2) of lherzolites, harzburgites and dunites from the Nain, Neyriz, Khoy, Esfandagheh and Fannuj ophiolitic complexes were compiled from several literature sources (Eslami *et al*. 2018; Shirdashtzadeh *et al*. 2017; Torabi 2001; Ghazi *et al*. 2011; Zaeimnia *et al*. 2017; Monsef et al. 2010Rajabzadeh *et al*. 2013; Sepidbar *et al*. 2021; Peighambari *et al*. 2011; Sepidbar *et al*. 2020). These peridotites show loss on ignition (LOI) contents that vary from 0.6 wt. % to 10.8 wt. %, indicating variable degrees of serpentinization. For this reason, the major oxides were normalized to 100% anhydrous; Supplementary Table S2). Nain peridotites have narrow ranges of SiO_2 (41–44 wt. %), Al_2O_3 (1.1–3.2 wt. %), MgO (41–47 wt. %) and TiO_2 (0.01–0.04 wt. %), but wide ranges of CaO (0.7–6.5 wt. %). They show variable CaO/Al_2O_3 ratios (0.4–6.1), and high Cr (1732–4119 ppm) and Ni (993–2097 ppm) contents. Neyriz and Khoy peridotites show variable SiO_2 (40.7–47.3 wt. %), Al_2O_3 (0.2–2.2 wt. %), CaO (0.06–2.2 wt. %), and TiO_2 (up to 0.04 wt. %) contents. Their CaO/Al_2O_3 ratio ranges from 0.3 to 2.1 and MgO ranges from 41 to 49 wt. %. They also have high Cr (889–3220 ppm) and Ni (1406–2731 ppm) contents. These compositions reflect the depleted nature of Iran ophiolite peridotites.

Esfandagheh ophiolite peridotites show variable SiO_2 (40.1–45.8 wt. %), MgO (40.3–49.4 wt. %), Al_2O_3 (0.5–2.5 wt. %), CaO (0.2–3.1 wt. %), and TiO_2 (0.01–0.06 wt. %) contents, with CaO/Al_2O_3 values from 0.6 to 2.5, and high Cr (2420–3090 ppm) and Ni (1260–2490 ppm) contents. Fannuj ophiolite peridotites have SiO_2 (42.7–44.8 wt. %), MgO (42.9–44.9 wt. %), Al_2O_3 (1.4–2.5 wt. %), CaO (0.9–1.7 wt. %), TiO_2 (0.01–0.04 wt. %) and Ni (2180–2097 ppm) contents and a narrow range of CaO/Al_2O_3 ratios (0.4–1.2). Peridotites from all regions in this study mostly plot within or close to terrestrial mantle (Figure 6a), showing that serpentinization has not affected major oxide contents, such as SiO_2, Al_2O_3 and MgO.

Chondrite (CI)-normalized REE (Sun and McDonough 1989) patterns (Figure 7) of peridotites from Nain, Khoy, and Neyriz ophiolites differ. For example: (1) Khoy peridotites are defined by flat REE patterns and have higher LREE and MREE values; (2) Khoy and Nain peridotites display strong La and Ce enrichment, which is very weak in those of Neyriz (Figure 7) and lack an Eu anomaly; (3) peridotites from the Fannuj area have relatively flat patterns from LREE to HREE (Figure 7), and also lack an Eu anomaly. However, in contrast to the others, Esfandagheh harzburgites show U-shape patterns with clear Eu anomalies (Figure 7).

4.3 Mantle oxidation state and thermometry

Nain peridotites show variable oxidation states, with log fO_2 units and temperatures ranging from +1.85 to +3.04 and 768°C to 877°C, respectively, for lherzolites; +0.45 to 2.4 and 691°C to 1021°C, respectively, for harzburgites; +2.60 to +3.55 and 882°C to 932°C, respectively, for dunites (Supplementary Table S3)

Khoy complex peridotites display variable oxidation states and temperatures, with wide ranges of log fO_2 from −0.05 to +0.89 and 755°C to 912°C, respectively, for lherzolites; −1.62 to +1.35 and 742°C to 914°C, respectively, for harzburgites. Both fO_2 and temperature generally increase from lherzolites to harzburgites (Supplementary Table S3).

The Neyriz and Esfandagheh ophiolitic peridotites are more oxidized, with log fO_2 units and temperatures ranging from −0.33 to +3.01 and 798°C to 970°C, respectively, for the lherzolites; −1.3 to +3.4 and 711°C to 796°C, respectively, for the harzburgites; and −0.2 to +3.8 and 769°C to 950°C, respectively, for the dunite (Supplementary Table S3).

Fannuj ophiolitic peridotites are oxidized, with log fO_2 units and temperatures ranging from +3.1 to +3.6 and 683°C to 846°C, respectively, for lherzolites; +1.7 to +3.5 and 728°C to 812°C, respectively, for harzburgites (Supplementary Table S3). The fO_2 and temperatures also increase from lherzolites to harzburgites, and plot above the upper limit of the continental-arc peridotite field (Supplementary Table S3).

5. Discussion

Primary spinel Cr# and Mg# compositions and whole-rock geochemistry of peridotites are used here to investigate the geodynamic evolution of Iran ophiolites. Spinel Cr# and Mg# can be used to indicate the degree of partial melting of an assumed primitive peridotite (e.g. Arai 1992). However, the Mg# of mantle minerals in the presence of Fe-rich minerals like spinel can change during heating and cooling due to Mg–Fe diffusive exchange, so the mineral pairs these are based on should be examined to ascertain that they are primary. Therefore, we used whole-rock and spinel-olivine geochemical data from Late Mesozoic Iranian ophiolites to interpret (1) subsolidus chemical changes in mantle minerals, (2) petrogenesis of different Iranian ophiolite peridotites, (3) petrogeochemical similarities and differences between Iranian ophiolites, and (4) decipher the geodynamic evolution of Iran during the Late Mesozoic.

5.1 Subsolidus chemical change of mantle minerals

The Mg and Fe contents of primary olivine and spinel in mantle rocks change during decompression and cooling due to intercrystalline and intracrystalline diffusion (e.g. Arai, 1992; Khedr and Arai 2013). Changes in mineral composition are affected by several factors, including mineral proportions, formation (or not) of exsolution structures, cooling rate, and re-equilibration temperatures (e.g. Arai 1992; Khedr and Arai 2013; Khedr *et al.* 2022). The investigated spinels mostly have primary compositions based on their morphology (vermicular shape), homogenous red colour in thin section (without zonation) and low MnO (mainly < 0.3 wt. %) and TiO_2 (<0.05 wt. %) contents, coupled with high Fe^{2+}/Fe^{3+}ratio

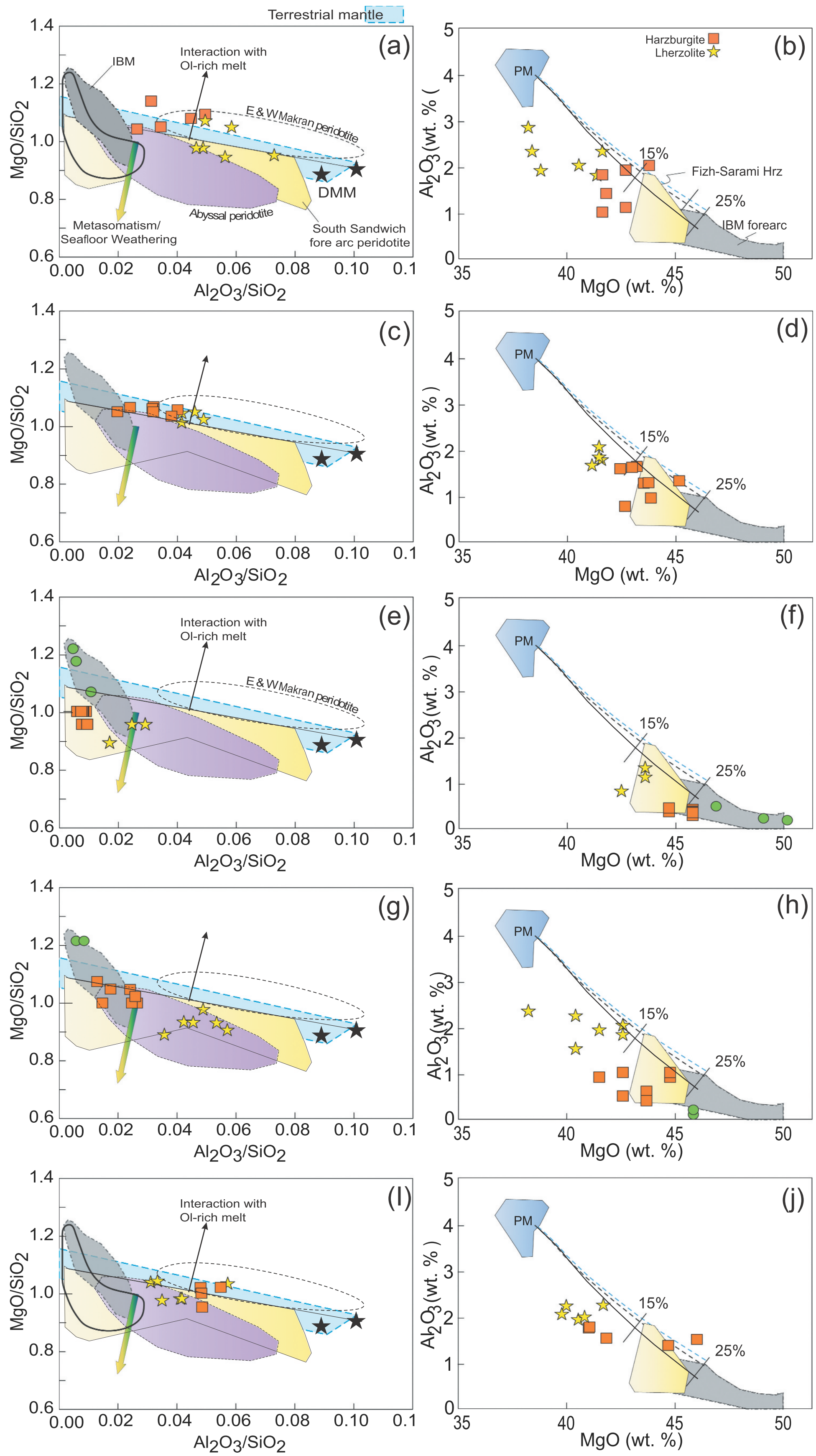

Figure 6. Peridotite compositions. Al_2O_3/SiO_2 vs MgO/SiO_2 (a,c,e,g,i) and Al_2O_3 versus MgO (b,d,f,h,j) diagrams (after Jagoutz et al. 1979; Hart and Zindler, 1986; Barnes et al. 2014; Lian *et al*. 2019; Nouri et al. 2019) for the Nain, Khoy, Neyriz, Esfandagheh, and Fannuj

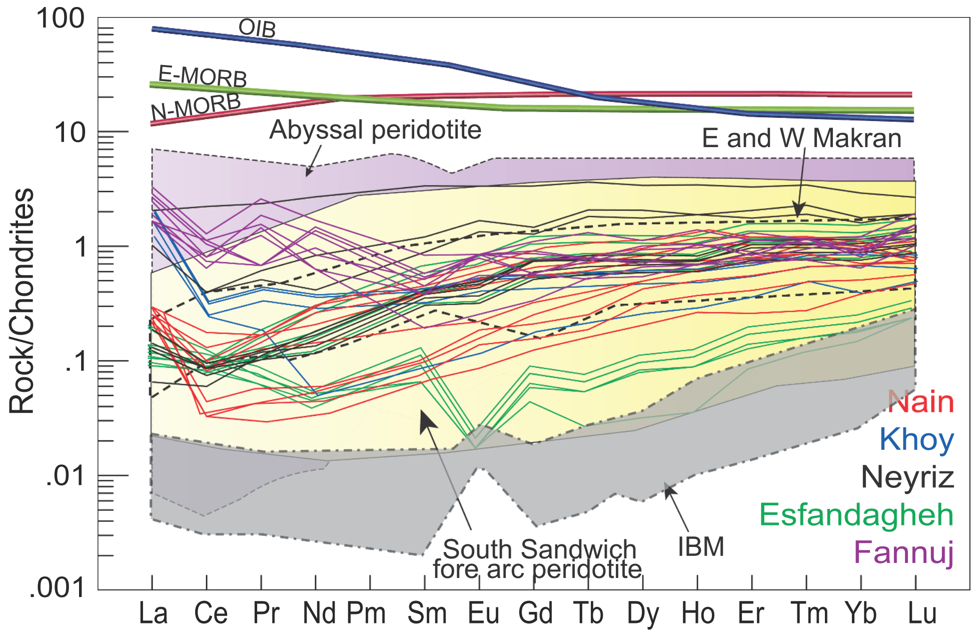

Figure 7. Chondrite-normalized rare earth element (REE) diagrams (.Sun and McDonough 1989) for Nain, Khoy, Neyriz, Esfandagheh, and Fannuj peridotites. Data for OIB, N-MORB, and E-MORB are after Sun and McDonough (1989), Eastern-Western Makran (E–W Makran) peridotites are after Monsef *et al*. (2019) and Sepidbar *et al*. (2020), abyssal peridotites are after Niu *et al*. (1997) and Lian *et al*. (2019), and South Sandwich forearc peridotites are after Pearce *et al*. (2000)

(>5) (Supplementary Table S1), like primary spinels in other ophiolitic mantle sections (e.g. Khedr *et al*. 2014, 2022). It should be mentioned that Cpx Mg# has been significantly enhanced by Mg-Fe exchange with abundant olivine. Mg and Fe of spinel mainly changed via diffusion between olivine (and opx) and spinel based on the modal volume of these minerals. Therefore, spinel Mg/Fe ratios may also change due to cation exchange with olivine (olivine prefers Mg and spinel prefers Fe) during subsolidus diffusional modification (Arai 1992, 1994), so these ratios should not be used as petrogenetic indicators. Even in this case, Cr# and TiO_2 (Figures 4, 8) content may be intact and reflect its primary compositions and can be used as petrogenetic indicators. Combined olivine Fo versus spinel Cr# is a better petrogenetic indicator (Figure 8). No chlorite around primary spinel (as corona texture) in thin sections was observed; consequently, Al from spinel was not consumed to form chlorite and no significant Al-Cr changes in spinels are inferred. Cr/Al in spinels range mainly < 1.8 for Nain, < 2.8 for Khoy, < 2.5 for Neyriz, < 2.9 for Esfandagheh and < 2 for Fannuj; Supplementary Table 1), resembling the Cr/Al range of Oman ophiolitic peridotite spinels (Cr/Al: 0.08–1.6 after Khedr *et al*. 2014) and primary spinel (Cr/Al: 1.2–2.8) in Neoproterozoic serpentinized peridotites (Khedr *et al*. 2022). There are no exsolution textures in pyroxene and spinel and there is little variation in their compositions due to low modal volume proportions in peridotites. Pyroxenes do not show exsolution textures and no change in Ca content of pyroxenes. Tschermak's components (Al and Cr contents) of spinel show little variation due to the absence of exsolution. However, Mg# of cpx and spinel in peridotites may have changed because of their low abundances.

Excellent preservation of primary spinel compositions may reflect rapid cooling, potentially due to the addition of large volumes of slab-derived fluids that elevated fO_2 (Supplementary Table S3) (e.g. Khedr *et al*. 2022). Primary olivine in Nain, Khoy, Neyriz, Esfandagheh, and Fannuj peridotites with unmodified textures

peridotites (after Ishii *et al*. 1992; Moghadam *et al*. 2013; Moghadam and Stern 2015; Monsef *et al*. 2019). Mantle depletion trend, fields of abyssal peridotites, and forearc peridotites are from Pearce *et al*. (1992). Depleted MORB Mantle (DMM: Workman and Hart 2005), primitive mantle (PM; Sun and McDonough 1989), abyssal peridotite (Niu *et al*. 1997), forearc peridotite (Parkinson and Pearce 1998), metasomatism/seafloor weathering trend (Paulick et al. 2006), interaction with olivine-rich melts, and terrestrial array (Jagoutz et al. 1979) are shown. Note systematic correlations, reflecting partial melting between 15% and 25% by either isobaric batch melting (broken line) or near-fractional polybaric melting (solid line) (e.g. Niu *et al*. 1997). PM: primitive mantle; Fizh-Sarami Hrz: Fizh-Sarami (Oman) harzburgite. Data for the IBM forearc, Fizh-Sarami Hrz and PM are from Khedr *et al*. (2014) and references therein.

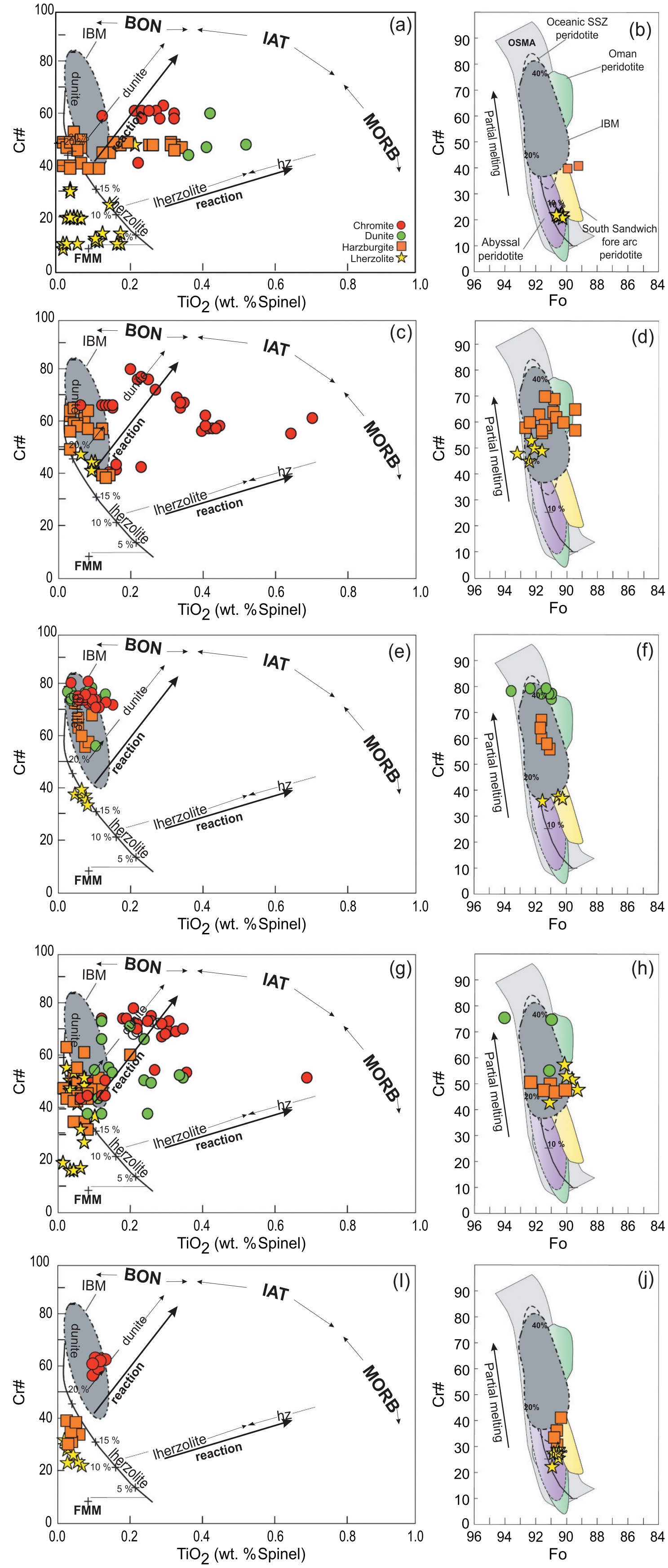

Figure 8. TiO_2 vs. Cr# and Mg# vs. Cr# diagrams for spinel (Pearce *et al.* 2000) for the (a-b) Nain, (c-d) Khoy, (e-f) Neyriz, (g-h) Esfandagheh and (i-j) Fannuj ophiolites. Spl: spinel.

nonetheless show no evidence of changed chemical compositions due to Fe-Mg exchange with spinel; this reflects the abundance of olivine and scarcity of spinel in each lithology. This is confirmed by the investigated olivine Mg# (0.89–0.91, 0.89–0.91, 0.91–0.94, 0.89–0.94, and 0.9–0.91) (Supplementary Tables S1, S2) that are similar to primary mantle olivine Mg# in other fresh mantle peridotites (Takahashi *et al*. 1987; Khedr *et al*. 2014). In addition, the investigated Mg# of Nain, Khoy, Neyrize, Esfandagheh, and Khoy peridotites (0.90–0.92, 0.90–0.91, 0.90–0.92, 0.90–0.91, and 0.91–0.92) is consistent with their olivine Mg# values (0.89–0.91, 0.89–0.91, 0.91–0.94, 0.89–0.94, and 0.9–0.91), suggesting no changes in chemical compositions during Fe-Mg exchange between olivine and spinel.

Examined olivines in the Nain, Khoy, Neyriz, Esfandagheh, and Fannuj peridotites plot in and around the olivine mantle array (Takahashi *et al*. 1987) (Figure 5), reflecting their primary origin and little chemical changes during Fe-Mg exchange between olivine and spinel because of the small amount of spinel. Olivine Mg# in peridotite is almost constant because of its great abundance. In addition, olivines in the Nain, Khoy, Neyriz, Esfandagheh, and Fannuj peridotites show primary textures and lack opaque inclusions (characteristic of metamorphic olivine; Khedr and Arai 2012) and have compositions ($Fo_{89–90}$, NiO < 0.39 wt. %, MnO = 0.08–0.16 wt. %; $Fo_{89–91}$, NiO < 0.44 wt. %, MnO = 0.09–0.21 wt. %; $Fo_{91–94}$, NiO < 0.66 wt. %, MnO of up to 0.13 wt. %; Fo_{89-94}; NiO = 0.32–0.58 wt. %; MnO = 0.09–0.18 wt. %; and $Fo_{90.6–92.2}$; NiO = 0.39 wt. %, MnO = 0.13 wt. %, respectively) that are similar to primary mantle olivine (Arai, 1992; Takahashi *et al*. 1987) and primary olivine in Oman ophiolitic harzburgites (Khedr *et al*. 2014). Because most of the investigated Cr-spinels, olivines, and orthopyroxenes show primary textures, lack opaque inclusions, and do not extend to high Fo (Fo>95) contents characteristic of metamorphic olivine (Khedr and Arai 2012), we conclude that Iran ophiolite peridotite olivines and spinels are primary and are important petrogenetic indicators of their host peridotite formation.

5.2. Petrogenesis of late mesozoic Iran ophiolites

The Al_2O_3 vs. MgO contents of the five ophiolitic peridotites show approximately the same trend with either isobaric batch melting (dashed line) or near-fractional polybaric melting (solid line) trends (Figure 6b). However, they plot far from the melting curve which suggests that the original mantle was more depleted than primitive mantle (PM). From this diagram, 10–15% melting of Iran ophiolitic lherzolites is inferred (except Neyriz lherzolite, which shows around 17% partial melting), 15–20% melting for harzburgites (except Neyriz harzburgites which shows around 23% partial melting) and >25% partial melting for dunites. The degrees of peridotite partial melting from the investigated ophiolites can also be estimated based on spinel chemistry (Pearce *et al*. 2000), which indicates (i) ~5–20% melting for lherzolites and around 20% for Nain and Esfandagheh harzburgites; (ii) ~15–17% melting for lherzolites and 22–25% for harzburgites from Khoy and Neyriz; and (iii) 10–15% melt fraction for lherzolites and 15–18% for harzburgites from the Fannuj ophiolite (Figure 8). Although spinels in dunites and chromitites tend to show boninitic signatures, melt-rock reactions show less effect in Neyriz and Fannuj dunites and chromitites (Figure 8).

Nain and Esfandagheh lherzolites and harzburgites show ~5–25% partial melting, whereas those from Khoy and Neyriz show 15–18% partial melting (Figure 6). The residual mantle signature in these units, relative to PM (Sun and McDonough 1989; Workman and Hart 2005) and depleted MOR mantle (DMM) values (Workman and Hart 2005), is suggested by their high Ni, Cr, MgO and low incompatible element contents (e.g. Ohara *et al*. 2002), along with depletion in TiO_2, CaO and Al_2O_3 for both the bulk rock and individual spinels (e.g. Pearce *et al*. 2000; Khedr *et al*. 2010, 2014). Moreover, mantle residues after moderate degrees of melt extraction show higher MgO/SiO_2 and lower Al_2O_3/SiO_2 ratios than those of PM (Workman and Hart 2005) and DMM (Workman and Hart 2005) (Lian *et al*. 2019) (Figure 6).

Peridotite minerals (e.g. spinel) are expected to have the same composition as the first phases (e.g. spinel, olivine) precipitated from extracted magmas (Arai 1994). Lherzolite spinels of Nain, Khoy, Neyriz, Esfandageh, and Fannuj, and Fannuj harzburgites show chemical characteristics of spinels in residual peridotites. In contrast, dunite and chromitite spinels of the Khoy, Esfandagheh, and Neyriz ophiolites show boninitic signatures (Figure 4). Spinels in residual harzburgites from Nain, Khoy, Neyriz, and Esfandagheh ophiolites are primary mantle minerals that re-equilibrated with boninitic melts, and so are similar to chromian spinels in arc-related peridotites (Arai and Ishimaru 2008; Arai *et al*. 2011; Khedr and Arai 2017) (Figure 1). Such residual spinels are chemically similar to spinels crystallized from boninitic melts and may record chemical signatures of re-equilibrating with tholeiitic or boninitic melts during peridotite–melt interactions.

These distinctions are emphasized in a TiO_2 vs. Cr# diagram, where lherzolite spinels from Nain, Khoy, Neyriz, Esfandagheh, and Fannuj ophiolites plot in the field of depleted peridotites (Figure 8). Nain and

Esfandagheh peridotite spinels plot in the overlapping field of MOR and arc spinels, but Khoy, Neyriz and Esfandagheh dunite–chromitite spinels have compositions similar to boninitic spinels (Figure 8), suggesting a change from early proto-forearc spreading to generate tholeiites to late proto-forearc magmatism to generate boninites. Spinel chemistry of Nain, Neyriz, and Fannuj lherzolites resemble those of depleted peridotite, indicating these were in equilibrium with tholeiitic or MOR peridotite melts (Supplementary Table S1), suggesting their generation during partial melting to form tholeiitic- or MORB-like melts associated with proto-forearc spreading. This distinction is also clear in the Cr# vs. Mg# (Figure 4) and TiO_2 vs. Cr# diagrams (Figure 8), where the lherzolite spinels of these regions plot in the field of depleted peridotites. In contrast, the melts in equilibrium with harzburgite-dunite-chromitite from Nain and harzburgite-chromitite of Fannuj resemble those of forearc basalts (FAB) (Supplementary Table S3), suggesting their generation during the proto-forearc stage. However, FAB signatures of these equilibrium melts increase from harzburgite to chromitite, which agrees with their spinel chemistry in Cr# vs. Mg# (Figures 4, 8) and TiO_2 vs. Cr# diagrams (Figure 8), where the dunite–chromitite spinels of Nain and harzburgite-chromitites of Fannuj ophiolites show minor reaction trends, respectively. More precisely, the composition of the Nain and Fannuj ophiolites chromitites is consistent with the reaction trend proposed by Pearce *et al*. (2000).

Calculated fO_2 data for Nain and Fannuj lherzolites are similar to those of continental arc peridotites, whereas those of harzburgites and dunites correlate with oceanic-arc peridotites (Figure 9), which is expected for an oxidized SSZ mantle wedge (Pearce *et al*. 2000). Chromitites and associated dunite envelopes show higher fO_2 than associated harzburgites. The increase in fO_2 from harzburgites to dunites is interpreted as recording progressive interactions between residual mantle harzburgite (with MOR or FAB signatures) and higher-fO_2 SSZ melts, which produce dunites owing to the hydrous nature of SSZ melts (e.g. Ishii *et al*. 1992; Parkinson and Pearce 1998; Pearce *et al*. 2000; Dare *et al*. 2009). Such a process may be interpreted from chemical trends on a TiO_2 vs. Cr# diagram (Figure 8).

Khoy lherzolites record lower degrees of partial melting (10–15%; Figure 8) and these melts inferred from spinel compositions are similar to tholeiitic or MOR melts. This suggests generation by partial melting during back-arc extension, perhaps associated with subduction initiation (Moghadem and Stern 2021). This is corroborated by spinel compositions on Cr# v. Mg# (Figure 4) and TiO_2 vs. Cr# diagrams (Figure 8). Parent melts of Khoy ophiolite harzburgites–chromitites are similar to BAB or FAB (Supplementary Table S1). This agrees with spinel chemistry shown in Cr# vs. Mg# (Figure 4) and TiO_2 vs. Cr# diagrams (Figure 8). The fO_2 of Khoy ophiolite lherzolites and harzburgites overlap with continental, forearc, arc and abyssal peridotite fields (Figure 9), being equivalent to an oxidized SSZ mantle setting (Pearce *et al*. 2000). The wide range of log fO_2 (−1.6 to +5.6) of Khoy ophiolitic peridotites suggests that interaction between residual mantle rocks (with lower fO_2 values) and SSZ melts (with higher fO_2 values) produced harzburgite owing to the hydrous nature of the SSZ melts (e.g. Ishii *et al*. 1992), in agreement with how these plot on the TiO_2 vs. Cr# diagram (Figure 8)

Neyriz and Esfandageh lherzolites record low to moderate degrees of partial melting (~15–20% and 7–17% melting, respectively; Figure 8) suggesting generation in a proto-forearc. This is supported by Cr# vs. Mg# (Figure 4) and TiO_2 vs. Cr# diagrams (Figure 8), where the lherzolite spinels of Neyriz and Esfandageh ophiolites plot in the field of depleted peridotites. Neyriz and Esfandageh harzburgites record ~22–30% partial melting (Figure 8) and their spinel chemistry and parent melts are in equilibrium with FAB, also suggesting their generation beneath a proto-forearc. This is supported by the Cr# vs. Mg# diagram (Figure 4), where the harzburgite spinels of Neyriz and Esfandageh ophiolites lie in the forearc peridotite field. In contrast, the parent melts of spinel in dunite and chromitite from these ophiolites have boninitic signatures (Supplementary Table S1a-e), suggesting their generation during subduction initiation. This is in agreement with spinel chemistry in Cr# vs. Mg# (Figure 4) and TiO_2 vs. Cr# diagrams (Figure 8), where the dunite–chromitite spinels of Neyriz and Esfandagheh ophiolites show boninitic and reaction chromite trends. The fO_2 of all the lherzolites, harzburgites, and dunites from the Neyeriz and Esfandagheh ophiolites plot at the border of oceanic-arc peridotites (Figure 9), equivalent to the mantle wedge in an oxidized SSZ setting (Pearce *et al*. 2000). The fO_2 and temperatures of the Neyriz and Esfandagheh units also increased from lherzolites to dunites (Figure 8), confirming that their interactions also produced dunite (e.g. Ishii *et al*. 1992), in agreement with their position in a TiO_2 vs. Cr# diagram (Figure 8).

Thus, all investigated peridotites have characteristics of a forearc or a back-arc basin setting consistent with their location relative to the palaeo-Zagros trench. Their compositions are consistent with formation as residues during partial melting associated with subduction initiation (Moghadem and Stern 2021). As such, there are large variations in degrees of partial melting (5–30%; Figure 4), a wide range of oxygen fugacity (−1.6 to +5.6 log units) and changes of magma

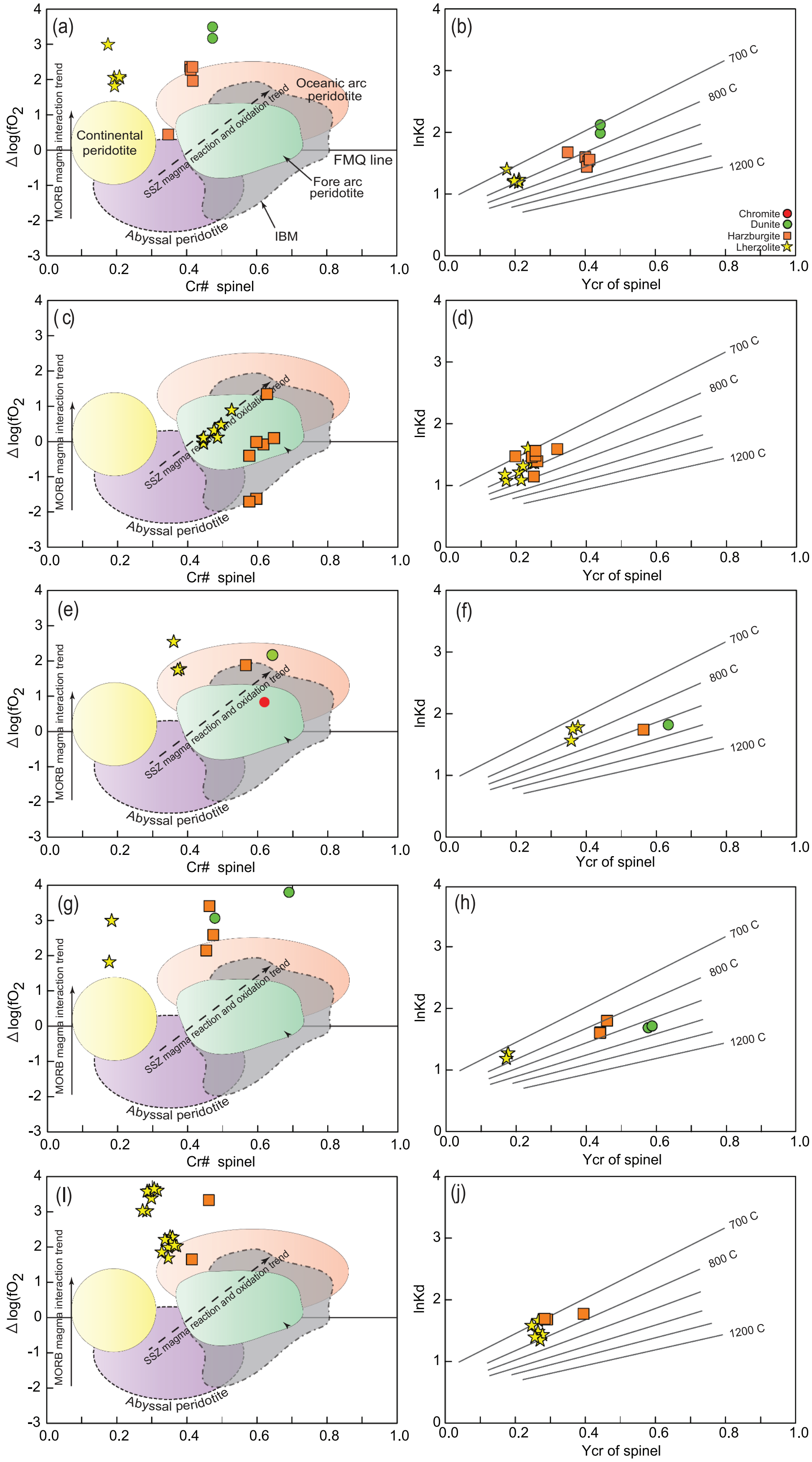

Figure 9. Plot of oxygen fugacity as ΔlogfO_2 vs. Cr# of chromian spinels and two-pyroxene thermometry for the studied chromitites and associated ultramafic rocks of the (a-b) Nain, (c-d) Khoy, (e-f) Neyriz, (g-h) Esfandagheh, and (i-j) Fannuj ophiolitic complexes. The tectonic discrimination fields of abyssal (MORB) peridotites, fore-arc peridotites, oceanic-arc peridotites and continental peridotites are adopted from Parkinson and Pearce (1998). The solid and dashed arrows denote the trends for residual peridotite compositions interacting with MORB and supra-subduction zone (SSZ) melts, respectively. Note that all the data lie above the FMQ buffer line.

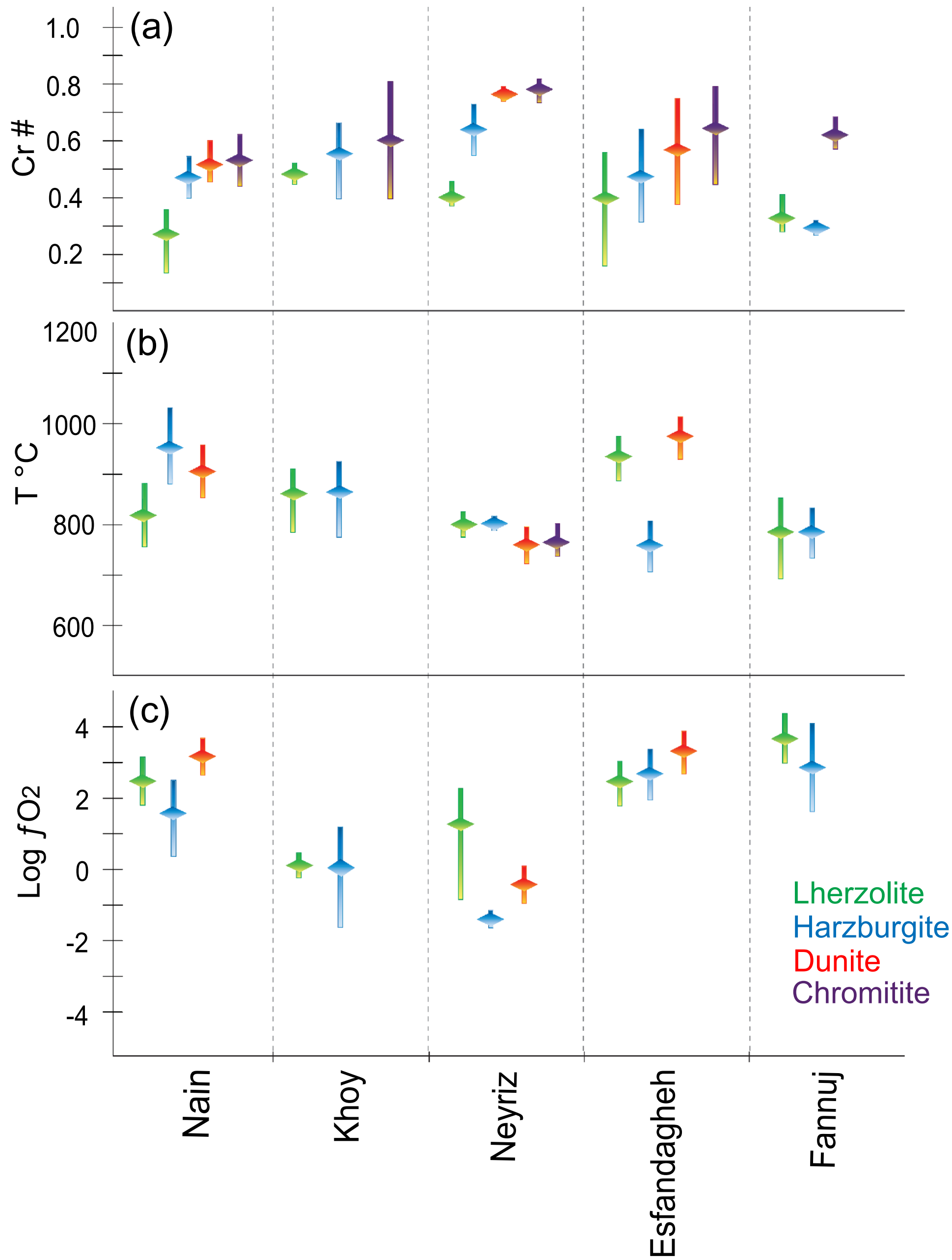

Figure 10. Simplified chart showing the range of Cr#, equilibrium temperatures and fO_2 for mantle sequences of the Mesozoic ophiolites. Nain mantle sequence data (Supplementary Tables S1, S2) are after Eslami *et al*. (2018), Shirdashtzadeh *et al*. (2017), Torabi (2001) and Ghazi *et al*. (2011). Neyriz, Esfandagheh, and Khoy mantle sequence data (Supplementary Table S1, S2) are after Zaeimnia *et al*. (2017), Monsef *et al*. (2010), Rajabzadeh *et al*. (2013), Sepidbar *et al*. (2021), and Peighambari *et al*. (2011); and Fannuj mantle sequence data are after Sepidbar *et al*. (2020). Green diamonds: Lherzolite; Blue diamonds: Harzburgite; Red diamonds: Dunite; Purple diamonds: Chromirite.

compositions (Figure 9 and Supplementary Table S3) that partly reflect whether the ophiolites formed in the proto-forearc (Neyriz, Esfandagheh, Fannuj) or back-arc (Nain, Khoy; Figure 1).

Mantle fO_2 is controlled mostly by the addition via fluid infiltration of subducted oxidized crustal components into a moderately reduced asthenosphere (Ballhaus *et al*. 1990), so that the mantle wedge above a subducting slab is more oxidized than mantle in other geodynamic settings (e.g. Ballhaus *et al*. 1990; Palin *et al*. 2020). Olivine–spinel chemistry in the studied units shows that dunites have higher fO_2, temperatures and spinel Cr# than related lherzolites and harzburgites. The increase of Cr#, fO_2 and temperatures from lherzolite–harzburgites to dunites must therefore have occurred due to interactions between residual mantle harzburgites and SSZ-type hydrous melts (i.e. highly oxidizing condition and fO_2) (e.g. Ishii *et al*. 1992; Parkinson; Pearce *et al*. 2000; Dare *et al*. 2009). However, it seems that Khoy backarc ophiolitic complex formed under more variable fO_2 and temperature conditions relative to the Esfandagheh and Neyriz examples located in forearc positions during subduction initiation (Supplementary Table S3). Although the Esfandagheh and Fannuj ophiolites have similar fO_2 to the Nain ophiolite, they formed at lower equilibrium temperatures (Figure 9) (Supplementary Table S3). The low calculated equilibration temperature (~700°C) and high values of calculated fO_2 relative to that of arc peridotites (e.g. Pearce *et al*. 2000) are interpreted to represent the dominance of fluid metasomatism and cooling. The abundance of H_2O contents enhanced the oxidation of mantle wedge peridotites and forearc peridotites (Ballhaus *et al*. 1990, 1991; Khedr and Arai 2013, 2017), causing high fO_2. Similar equilibrium temperatures of <700°C have been documented from the Happo-O'ne (Japan) peridotites, thought to have formed near the corner of the mantle wedge overlying the slab at a depth of <50 km (Khedr and Arai 2010). This is in agreement with low temperature of mantle wedge peridotites (Davies 1999; Abers *et al*. 2006). It is also well known that enrichment of LREE in mantle rocks is due to pervasive metasomatism of peridotites by slab-derived fluids (e.g. Hernández-Uribe *et al*. 2020). La and Ce are more mobile and are enriched in fluids compared to other REE; however, La and Ce are highly sensitive to retrograde metamorphism and contamination, and so both errors during analyses or syn- or post-exhumation alteration of mantle rocks can lead to significantly higher La and Ce concentrations in ophiolite.

5.2 Petrogeochemical similarities and differences between Iranian ophiolites

Most Iranian Mesozoic ophiolites have similar Late Cretaceous ages, including 92–93 Ma for Outer belt Neyriz hornblende gabbros (^{40}Ar-^{39}Ar; Babaie *et al*. 2006); 103–99 Ma for Inner belt plagiogranites and diorites (U–Pb zircon; Moghadam *et al*. 2013), and 101–77 Ma for Khoy gabbros (Khalatbary Jafary *et al*. 2016). However, these ages are notably younger than those of the Makran (U–Pb zircon; 145–111 Ma), Kahnuj (Ar–Ar; 143–141 Ma) and Birjand (U–Pb zircon: 113–107 Ma for gabbros) ophiolites (Moghadam and Stern 2015). In particular, the Late Cretacous ophiolites are related to subduction initiation on the N side of the Neo-Tethys Ocean (Moghadem and Stern 2021).

The spinel compositions of the backarc Nain lherzolite, the Neyriz and Esfandagheh units from the outer ZOB, and lherzolite-harzburgite from Fanuuj show abyssal geochemical signatures (Supplementary Table S1; Figure 4). They are mostly Al-rich with low Cr#, similar to back-arc basin and/or abyssal peridotites (Figure 4a-o). However, Khoy lherzolite spinel compositions show abyssal and suprasubduction zone signatures (Supplementary Table S1a), whereby they plot near the Cr–Al line and are mostly richer in Cr than other Iran lherzolites (Figure 4). Lherzolite spinels have the same compositions in both forearc and backarc ophiolitic belts with abyssal peridotite affinity, suggesting similar sources during Early Cretaceous to Late Cretaceous for their genesis. Harzburgite spinels are also similar in composition for both inner and outer Zagros and Makran ophiolitic belts with abyssal and forearc affinity, suggesting similar sources. On the other hand, the spinel compositions of forearc Neyriz and Esfandagheh harzburgite (Figure 4b-c) show a stronger SSZ affinity than those of backarc Nain (Figure 4a-c) and Fannuj units from the Makran zone (Figure 4a-c). Dunite and chromitite from all regions plot in the overlapping space of both abyssal and forearc peridotites and are consistent with the reaction trend (Figure 8). Spinels in lherzolites and harzburgites show similar fabrics (i.e. symplectic spinel and exsolusion lamella of spinel in orthopyroxene and clinopyroxene) in both the inner and outer Zagros and Makran ophiolitic belts; however, small differences in the chemical composition of Cr-spinel and olivine indicate formation from a similar mantle source. Because inner and outer Zagros ophiolites have the same geochemical and spinel chemistry as those of the Makran ultramafics (Figure 4, 5, 6, 10), we infer that lherzolites and less depleted Nain, Neyriz and Fannuj harzburgites are associated with similar subcontinental-upper mantle materials that show MOR peridotite characteristics or have early proto-arc spreading features. Moreover, metasomatized peridotites (harzburgite, dunite, and chromitite) from these ophiolites suggest that their protoliths were trapped and modified in a mantle wedge environment before exhumation. This is expected for peridotites related to subduction initiation.

Whole-rock geochemistry of ultramafic components of Iranian ophiolites also confirm that the lherzolites likely originated from a slightly metasomatized mantle, with slight enrichment in LILEs (i.e. Sr, Ba, Pb, Cs, U) and depletion of HFSEs indicating a mantle source associated with an early-stage proto-arc. Chromite deposits and their dunite envelopes are surrounded predominantly by residual dunite formed from interaction between boninitic melts and harzburgites later during subduction initiation. Moreover, the SSZ-type affinity of peridotites is clearer among the forearc ophiolites Neyriz and

Esfandagheh ophiolites) than those of the backarc (Khoy and Nain) and Fannuj ophiolites.

5.3 Geodynamic evolution of late mesozoic Iranian ophiolites

Our compiled geochemical data for these lherzolites confirm the presence of Neo-Tethys MOR oceanic lithosphere along the ZOB and ZIB. ZOB ophiolites are located between older rocks of the Sanandaj-Sirjan zone and the Main Zagros thrust fault, in a forearc setting. ZIB ophiolites have been recognized as forming from a Neo-Tethys oceanic branch between the Sanandaj-Sirjan zone and the Lut block (e.g. Arvin and Robinson 1994). It is suggested that the Nain-Baft ophiolite belt represents a suture of this Neo-Tethys oceanic branch (e.g. Agard *et al*. 2005; Moghadam *et al*. 2009). However, the occurrence of turbidites suggests that ZIB ophiolites formed near a rifted margin, where deep-water radiolarites, platform carbonates, and rift-related alkaline lavas are absent (Moghadam and Stern 2015).

Some researchers suggest a Campanian back-arc origin for ZIB ophiolites (e.g. Agard *et al*. 2006; Moghadam *et al*. 2009), whereas others suggest a subduction initiation/infant-arc model origin (Moghadam and Stern 2011). In the latter model, Late Cretaceous Zagros ophiolites are remnants of a long, broad, and continuous tract of oceanic lithosphere formed during subduction initiation along the southern margin of Eurasia. This subduction initiation event was accompanied by extension and early arc igneous activity, which initially occurred via seafloor spreading to form residual lherzolites (Moghadam and Stern 2015). Moghadem and Stern (2021) concluded that similar signatures of ZIB and ZOB lherzolites formed due to similar melting as a result of broad extension that accompanied subduction initiation. This model is supported by strong SSZ affinities of most Zagros ophiolite igneous rocks, especially for the most diagnostic lithologies of mantle harzburgites, and by the observation of early MORB-like lavas in some of these ophiolites, which are succeeded by more arc-like lavas (Whattam and Stern 2011). Some ZIB ophiolites are conformably overlain by arc-derived pyroclastic rocks. Mineral compositions and whole-rock geochemistry show that lherzolites from all regions and harzburgites of Nain, Neyriz and Fannuj lie close to the fields of MOR peridotites generated in an extensional environment or plot in the overlapping space of MOR peridotites and forearc peridotites (Figures 6, 7 and 8). This supports the presence of an extensional environment for Mesozoic lherzolites and harzburgites during proto-forearc spreading accompanying subduction initiation (Figure 11a,b). Our compiled data also indicate that forearc ophiolites have a stronger boninitic signature than back-arc ophiolites and those from the Makran zone, as expected for subduction initiation ophiolites.

Chromian spinels in the high-Cr dunite envelopes and chromitites are geochemically similar to spinels that formed in both boninite-forming late SI and in a mature SSZ setting (Figures 6–8; Supplementary Table S1; Kamenetsky *et al*. 2001; Parkinson and Pearce 1998; Pearce *et al*. 2000; Khedr and Arai 2013, Khalatbari Jafari *et al*. 2016, Khedr and Arai 2017). This indicates an SSZ origin for these chromitites (e.g. Khedr and Arai 2016, 2017). Spinel compositions of peridotites and associated chromitites plot near the Cr–Al line on the Cr–Al–Fe ternary diagram and show variable Cr and low Fe^{3+} contents (Figure 4). Such high-Al (with Av. Cr# of 0.42, 0.43, 0.49 and 0.57 for the Nain, Khoy, Esfandagheh and Fanuj, respectively) and high-Cr chromitites (with Av. Cr# of 0.61, 0.66, 0.73, 0.73 and 0.65 for the Nain, Khoy, Neyriz, Esfandagheh and Fanuj, respectively) can form in an arc-related setting during three stages; (i) early subduction initiation for lherzolites which are most consistent with a FAB-like melt; (ii) late subduction initiation stage for harzburgite formation that is most consistent with a boninite-like melt; and (iii) true subduction stage for chromitite formation. Most of the magmas in equilibrium with Cr-rich chromitites, except the Khoy region, experienced highly oxidizing conditions, with fO_2 values just above the FMQ buffer (Figure 9). All of these criteria suggest that the studied ophiolitic peridotites were depleted as a result of high degrees of partial melting in an SSZ setting. In contrast, Al-rich spinels in Khoy lherzolites have compositions resembling spinel in back-arc basin basalts (Zhou *et al*. 1998) with lower fO_2 values (Figure 9). These Al-rich spinels and host peridotites likely formed in an extensional environment during early proto-forearc spreading. Melts with a boninitic affinity formed in response to second-stage melting of previously depleted mantle later during subduction initiation, when large volumes of slab-derived water entered the mantle wedge beneath the fore-arc region (Khedr and Arai 2016, 2017; Palin and White 2016). Another way of saying this is that the lherzolites and harzburgites were re-fertilized due to percolating MOR-like tholeiitic melts beneath a proto-forearc spreading centre during subduction initiation and trench rollback stage (Moghadam *et al*. 2019), whereas the dunites reflect more extensive mantle melting as a result of a more hydrous environment (Figure 11).

We suggest that interaction of MORB-like melts with mantle peridotite precipitated low-Cr# chromitites in restricted domains. This is the mantle expression of the subduction initiation rule, articulated for well-studied ophiolite volcanic sections by Whattam and Stern (2011),

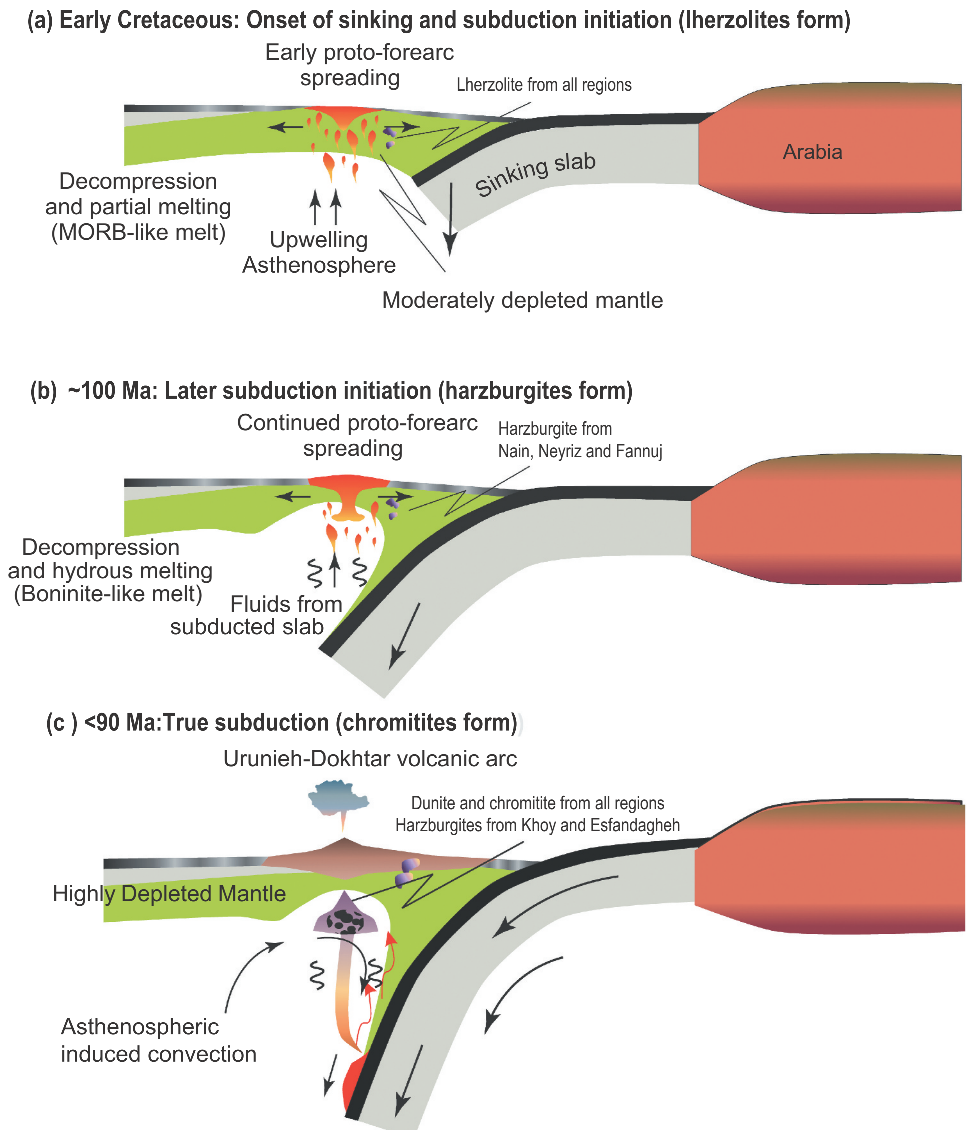

Figure 11. Schematic model for tectono-magmatic evolution and genesis of enriched peridotites, and high Cr# chromitites and dunitic rocks in the Mesozoic ophiolites of Iran.

whereby subduction initiation is manifested by early outpourings of tholeiitic (FAB: forearc basalt-) basalts followed by boninitic melts. Upwelling of asthenospheric mantle beneath the forearc region during the early stages of subduction initiation first resulted in decompression melting to form FAB and BABB (Reagan *et al*. 2010; Ishizuka *et al*. 2011). Such melts crystallized spinels with compositions like those of all Iran ophiolitic lherzolites and harzburgites of Nain, Neyriz and Fanuuj. Production of FAB melts during early-stage subduction initiation was followed by generation of arc-like or boninitic melts as slab-derived fluids flooded the zone of melt generation in the mantle wedge as the sinking slab descends further. These later boninitic melts formed Mesozoic dunites and high-Cr# chromitites from all regions (Figure 11). FAB-like melts are likely to be generated by extension-related melting in both the proto-forearc and backarc but the boninites are likely only in the proto-forearc because of reduced water flux with distance from the trench.

6. Conclusions

(1) Iran lherzolite spinels are geochemically characterized by a lower Cr# (0.17 to 0.40) and plot in an abyssal peridotite field, whereas spinel in harzburgite (Cr# = 0.40–0.50) and dunite–chromitite (Cr# > 0.50) shows geochemical affinities to FAB or MORB and boninites, respectively.

(2) Whole-rock compositions suggest that Iran lherzolites and harzburgites are residues after moderate-to-

high degrees of partial melting (~15% for lherzolite and 25% for harzburgite).

(3) The composition of primary olivine and spinel indicates that dunites formed at higher fO_2 and temperatures than those of surrounding lherzolites and harzburgites. This suggests that dunite-chromitite spinel crystallized from boninitic melts after high-degree partial melting of a depleted mantle source, but that lherzolite-harzburgite spinel is residual after moderate-degree partial melting of peridotite.

(4) Increases in spinel Cr#, fO_2, and equilibrium temperature of lherzolite-harzburgites to dunites are likely due to interactions between residual mantle harzburgites and SSZ melts enriched with H_2O, leading to highly oxidizing conditions and fO_2.

(5) The Late Cretaceous ophiolites of Iran are increasingly recognized as having formed in response to subduction initiation. Our results are consistent with that interpretation.

(6) Magma compositions, equilibrium temperatures and fO_2 varied within and between the Iranian ophiolite belts, but also evolved through Mesozoic in the same place due to the changes in tectonic style from proto-forearc arc to mature arc stages.

Acknowledgments

This is Postdoctoral research contribution #3471 funded by Ferdowsi University of Mashhad, Iran. We thank to Prof. Scott A. Whattam for editorial handling, Prof. Shoji Arai and anonymous reviewers for the positive comments and suggestions, improving the manuscript greatly. This is UTD Geosciences contribution # 1xxx.

Disclosure statement

No potential conflict of interest was reported by the author(s).

Funding

This work was supported by the Ferdowsi University of Mashhad [#3471].

References

Abbate, E., Bortolotti, V., and Principi, G., 1980, Apennine ophiolites: A peculiar oceanic crust. Ofioliti: p. 59–96.

Abers, G.A., van Keken, P.E., Kneller, E.A., Ferris, A., and Stachnik, J.C., 2006, The thermal structure of subduction zones constrained by seismic imaging: Implications for slab dehydration and wedge flow: earth planet: Sci. Lett, v. 241, p. 387–397

Agard, P., Monie, P., Gerber, W., Omrani, J., Molinaro, M., Meyer, B., Labrousse, L., Vrielynck, B., Jolivet, L., and Yamato, P., 2006, Transient, syn-obduction exhumation of Zagros blueschists inferred from P–T, deformation, time, and kinematic constraints: Implications for neotethyan wedge dynamics: Journal of Geophysical Research, v. 111, no. B11, p. B11401.10.1029/2005JB004103

Agard, P., Omrani, J., Jolivet, L., and Mouthereau, F., 2005, Convergence history across Zagros (Iran): Constraints from collisional and earlier deformation: International Journal of Earth Sciences, v. 94, no. 3, p. 401–419.10.1007/s00531-005-0481-4

Arai, S., 1992, Chemistry of chromian spinel in volcanic rock as a potential guide to magma chemistry: Mineralogical magazine. v. 56, p. 173–184.

Arai, S., 1994, Characterization of spinel peridotites by olivine-spinel compositional relationships: Review and interpretation: Chemical Geology, v.113, no. 3–4, p. 191–204.https://doi.org/10.1016/0009-2541(94)90066-3

Arai, S. 1997, Control of wall–rock composition on the formation of podiform chromitites as a result of magma/peridotite interaction: : Resource Geology, v. 47, no. p, p. 177–187.

Arai, S., and Ishimaru, S., 2008, Insights into petrological characteristics of the lithosphere of mantle wedge beneath arcs through peridotite xenoliths: A review: Journal of Petrology, v. 49, no. 4, p. 665–695.10.1093/petrology/egm069

Arai, S., and Miura, M., 2016, Formation and modification of chromitites in the mantle: Lithos, v. 264, p. 277–295.10.1016/j.lithos.2016.08.039

Arai, S., Okamura, H., Kadoshima, K., Tanaka, C., Suzuki, K., and Ishimaru, S., 2011, Chemical characteristics of chromian spinel in plutonic rocks: Implications for deep magma processes and discrimination of tectonic setting: : Island Arc, v. 20, no. 1, p. 125–137 10.1111/j.1440-1738.2010.00747.x

Arai, P.T., and Torabi, G.S., 2010, Post-deformational impregnation of depleted MORB in Nain lherzolite (Central Iran): Journal of Mineralogical and Petrological Sciences, v. 105, no. p, p. 74–79 10.2465/jmps.091014

Arvin, M., and Robinson, P.T., 1994, The petrogenesis and tectonic setting of lavas from the Baft ophiolitic mélange: Southwest of Kerman, Iran: Canadian Journal of Earth Sciences, v. 31, p. 824–834

Babaie, H.A., Babaei, A., Ghazi, A.M., Arvin, M., 2006, Geochemical, 40Ar/39Ar age, and isotopic data for crustal rocks of the Neyriz ophiolite, Iran: Canadian journal of earth sciences, v. 43, p.57–70.

Ballhaus, C., Berry, R.F., and Green, D.H., 1990, Oxygen fugacity controls in the earth's upper mantle: Nature, v. 348, no. 6300, p. 437–440 10.1038/348437a0

Ballhaus, C., Berry, R.F., and Green, D.H., 1991, High pressure experimental calibration of the olivine–orthopyroxene–spinel oxygen barometer: Implications for the oxidation state of the mantle: Contrib: Contributions to Mineralogy and Petrology, v. 107, no. 1, p. 27–40.10.1007/BF00311183

Barnes, J.D., Beltrando, M., Lee, C.T.A., Cisneros, M., Loewy, S., and Chin, E., 2014, Geochemistry of Alpine serpentinites from rifting to subduction: A view across paleogeographic domains and metamorphic grade: Chemical geology, v. 389, p. 29–47. 10.1016/j.chemgeo.2014.09.012

Dare, S.A.S., Pearce, J.A., McDonald, I., and Styles, M.T., 2009, Tectonic discrimination of peridotites using fO_2–Cr# and Ga–Ti–Fe^{III} systematic in chrome-spinel: Chemical Geology, v. 261, no. 3–4, p. 199–216.10.1016/j.chemgeo.2008.08.002

Davies, J.H., 1999, Simple analytic model for subduction zone thermal structure: Geophysical Journal International, v. 139, no. 3, p. 823–828.10.1046/j.1365-246x.1999.00991.x
Davoudzadeh, M., 1972, Geology and petrology of the area North of Nain, Central Iran. Geol. Surv. Iran. Rep., 1.
Dick, H.J.B., and Bullen, T., 1984, Chromian spinel as a petrogenetic indicator in abyssal and alpine-type peridotites and spatially associated lavas: : Contributions to Mineralogy and Petrology, v. 86, no. 1, p. 54–76.10.1007/BF00373711
Dilek, Y., and Furnes, H., 2011, Ophiolite genesis and global tectonics: Geochemical and tectonic fingerprinting of ancient oceanic lithosphere: Geological Society of America Bulletin, v. 123, no. 3–4, p. 387–411.10.1130/B30446.1
Dilek, Y., and Thy, P. 2009, Island arc tholeiite to boninitic melt evolution of the cretaceous kizildag (Turkey) ophiolite: Model for multi-stage early arc–forearc magmatism in Tethyan subduction factories: Lithos, v. 113, no. 1–2, p. 68–87.10.1016/j.lithos.2009.05.044
Eslami, A., Arai, S., Miura, M., and Mackizadeh, M.A., 2018, Metallogeny of the peridotite-hosted magnetite ores of the Nain ophiolite, central Iran: Implications for Fe concentration processes during multi-episodic serpentinization: Ore Geology Reviews, v. 95, p. 680–694.10.1016/j.oregeorev.2018.03.020
Ghazi, J., Moazzen, M., Rahgoshay, M., and Shafaii Moghadam, H., 2010, Mineral chemical composition and geodynamic significance of peridotites from Nain ophiolite, central Iran: Journal of Geodynamics, v. 49, no. 5, p. 261–270.10.1016/j.jog.2010.01.004
Ghazi, J., Moazzen, M., Rahgoshay, M., and Shafaii Moghadam, H. 2011, The geodynamic of the Nain ophiolitescentral Iran: Evidences from chromian spinel in the chromitites and associated rocks: Ofiliti, v. 36, no. v, p. 59–76.
Hart, S.R., and Zindler, A., 1986, In search of a bulk-earth composition: Chemical geology, v. 57, p. 247–267. 10.1016/0009-2541(86)90053-7
Hernández-Uribe, D., Hernández-Montenegro, J.D., Cone, K.A., and Palin, R.M., 2020, Oceanic slab-top melting during subduction: Implications for trace-element recycling and adakite Petrogenesis: Geology, v. 48, no. 3, p. 216–220.10.1130/G46835.1
Ishii, T., Robinson, P.T., Maekawa, H., and Fiske, R., 1992, Petrological studies of peridotites from diapiric serpentinite seamounts in the izu ogasawara mariana forearc. Leg 125 In: Fryer, P, Pearce, JA, Stokking, LB. (Eds.), Proceeding of Ocean Drilling Project: Scientific Results, v. 125, p. 445–485
Ishizuka, O., Tani, K., Reagan, M.K., Kanayama, K., Umino, S., Hariganen, Y., Sakamoto, I., Miyajima, Y., Yuasa, M., and Dunkley, D.J., 2011, The timescales of subduction initiation and subsequent evolution of an oceanic island arc: Earth and Planetary Science Letters. v. 229–240, p. 306. 10.1016/j.epsl.2011.04.006
Jagoutz, E., Palme, H., Baddenhausen, H., Blum, K., Cendales, M., Dreibus, G., Spettel, B., Wanke, H., and Lorenz, V., 1979, The abundances of major, minor and trace elements in the earth's mantle as derived from primitive ultramafic nodules: Lunar and Planetary Science Conference Proceedings, v. 10, p. 2031–2050.
Kamenetsky, V.S., Crawford, A.J., and Meffre, S., 2001, Factors controlling chemistry of magmatic spinel: An empirical study of associated olivine, Cr-spinel and melt inclusions from primitive rocks: Journal of Petrology, v. 42, no. 4, p. 655–671.10.1093/petrology/42.4.655
Khalatbari Jafari, M., Babaie, H.A., and Moslempour, M.E. 2016, Mid-ocean-ridge to suprasubduction geochemical transition in the hypabyssal and extrusive sequences of major upper cretaceous ophiolites of Iran: Geological Society of America Special Papers, v. 525, no. v, p. 525–527.
Khedr, M.Z., and Arai, S. 2010, Hydrous peridotites with Ti-rich chromian spinel as a low-temperature forearc mantle facies: Evidence from the Happo-O'ne metaperidotites (Japan): Contributions to Mineralogy and Petrology, v. 159, no. 2, p. 137.10.1007/s00410-009-0420-7
Khedr, M.Z., and Arai, S., 2012, Petrology and geochemistry of prograde deserpentinized peridotites from Happo-O'ne, Japan: Evidence of element mobility during deserpentinization: Journal of Asian Earth Sciences, v. 150–163, p.43.
Khedr, M.Z., and Arai, S., 2013, Origin of Neoproterozoic ophiolitic peridotites in south Eastern Desert, Egypt, constrained from primary mantle mineral chemistry: Journal of Mineralogy and Petrology, v. 107, no. 5, p. 807–828 10.1007/s00710-012-0213-y
Khedr, M.Z., and Arai, S., 2016, Chemical variations of mineral inclusions in neoproterozoic high-Cr chromitites from Egypt: Evidence of fluids during chromitite genesis: Lithos, v. 240–243, p. 309–326.10.1016/j.lithos.2015.11.029
Khedr, M.Z., and Arai, S., 2017, Peridotite-chromitite complexes in the eastern desert of Egypt: Insight into Neoproterozoic sub-arc mantle processes: Gondwana Research, v. 52, p. 59–79.10.1016/j.gr.2017.09.001
Khedr, M.Z., Arai, S., Python, M., and Tamura, A., 2014, Chemical variations of abyssal peridotites in the central oman ophiolite: Evidence of oceanic mantle heterogeneity: : Gondwana Research, v. 25, no. 3, p. 1242–1262.10.1016/j.gr.2013.05.010
Khedr, M.Z., Arai, S., Tamura, A., and Morishita, T., 2010, Clinopyroxenes in high-P metaperidotites from Happo-O'ne, central Japan: Implications for wedge-transversal chemical change of slab-derived fluids: Lithos, v. 119, no. 3–4, p. 439–456.10.1016/j.lithos.2010.07.021
Khedr, M.Z., Takazawa, E., Hauzenberger, C., Tamura, A., Arai, S., Stern, R.J., Morishita, T., and El-Awady, A., 2022, Petrogenesis of arc-related serpentinized peridotites (Egypt): Insights into Neoproterozoic mantle evolution beneath the Arabian-Nubian shield: Journal of Asian Earth Sciences, v. 226, p. 105078.10.1016/j.jseaes.2022.105078
Lian, D., Yang, J., Dilek, Y., and Rocholl, A., 2019, Mineralogy and geochemistry of peridotites and chromitites in the Aladag ophiolite (southern Turkey): Melt evolution of the cretaceous neotethyan mantle: Journal of the Geological Society, v. 176, no. 5, p. 958–974.10.1144/jgs2018-060
McCall, G.J.H., 1985, Explanatory text of the minab quadrangle map: Tehran, Geological Survey of Iran, p. 530. 1:250,000; No. J13
Moghadam, H.S., Corfu, F., Stern, R.J., and Bakhsh, A.L. 2019, The eastern Khoy metamorphic complex of NW Iran: A Jurassic ophiolite or continuation of the Sanandaj-Sirjan zone: Journal of the Geological Society, v. 176, no. 3, p. 517–529.10.1144/jgs2018-081
Moghadam, H.S., Li, X.H., Ling, X.X., Stern, R.J., Khedr, M.Z., Chiaradia, M., Ghorbani, G., Arai, S., and Tamura, A. 2015, Devonian to permian evolution of the paleo-tethys ocean: New evidence from U-Pb zircon dating and Sr–Nd–Pb isotopes of the Darrehanjir-Mashhad "ophiolites" NE Iran:

Gondwana Research, v. 28, no. 2, p. 781–799.10.1016/j.gr.2014.06.009
Moghadam, H.S., Mosaddegh, H., and Santosh, M. 2013, Geochemistry and petrogenesis of the late cretaceous Haji-Abad ophiolite (Outer Zagros ophiolite belt, Iran): Implications for geodynamics of the Bitlis–Zagros suture zone: Geological Journal, v. 48, no. 6, p. 579–602.10.1002/gj.2458
Moghadam, H., and Stern, R.J., 2011, Late cretaceous forearc ophiolites of Iran: Island Arc, v. 20, no. 1, p. 1–4.10.1111/j.1440-1738.2010.00745.x
Moghadam, H., and Stern, R.J., 2015, Ophiolites of Iran: Keys to understanding the tectonic evolution of SW Asia:(I) Paleozoic ophiolites: Journal of Asian Earth Sciences, v. 91, p. 19–38.10.1016/j.jseaes.2014.04.008
Moghadam, H., Whitechurch, H., Rahgoshay, M., and Monsef, I., 2009, Significance of nain-baft ophiolitic belt (Iran): Short-lived transtensional cretaceous back-arc oceanic basins over the Tethyan: Comptes Rendus Geoscience, v. 341, no. 12, p. 1016–1028.10.1016/j.crte.2009.06.011
Moghadem, H.S., and Stern, R.J., 2021, Subduction initiation causes broad upper plate extension: The late cretaceous iran example: Lithos, v. 398-399, p. 106296.10.1016/j.lithos.2021.106296
Monsef, I., Rahgoshay, M., Mohajjel, M., and Shafaii Moghadam, H., 2010, Peridotites from the Khoy Ophiolitic complex NW Iran: Evidence of mantle dynamics in a supra-subduction-zone context: Journal of Asian Earth Sciences, v. 38, no. 3–4, p. 105–120.10.1016/j.jseaes.2009.10.007
Monsef, I., Rahgoshay, M., Pirouz, M., Chiaradia, M., Grégoire, M., and Ceuleneer, G. 2019, The eastern makran ophiolite (SE Iran): Evidence for a late cretaceous fore-arc oceanic crust: International Geology Review, v. 61, no. 11, p. 1313–1339.10.1080/00206814.2018.1507764Niu
Niu, Y., Langmuir, C.H., and Kinzler, R.J., 1997, The origin of abyssal peridotites: A new perspective: Earth and planetary science letters, v. 152, no. 1–4, p. 251–265. 10.1016/251–265
Nouri, F., Asahara, Y., Azizi, H., and Tsuboi, M., 2019, Petrogenesis of the Harsin–Sahneh serpentinized peridotites along the Zagros suture zone, western Iran: New evidence for mantle metasomatism due to oceanic slab flux: Geological magazine, v. 156, no. 5, p. 772–800. 10.1017/S0016756818000201
Ohara, Y., Stern, R.J., Ishii, T., Yurimoto, H., and Yamazaki, T., 2002, Peridotites from the Mariana trough: First look at the mantle beneath an active back-arc basin: Contributions to Mineralogy and Petrology, v. 143, no. 1, p. 1–18.10.1007/s00410-001-0329-2
Pagé, P., Bédard, J.H., Schroetter, J.M., and Tremblay, A., 2008, Mantle petrology and mineralogy of the Thetford mines ophiolite complex: Lithos, v. 100, no. 1–4, p. 255–292. 10.1016/j.lithos.2007.06.017
Palin, R.M., Santosh, M., Cao, W., Li, S.S., Hernández-Uribe, D., and Parsons, A., 2020, Secular change and the onset of plate tectonics on Earth: Earth-Science Reviews, v. 207, p. 103172
Palin, R.M., and White, R.W., 2016, Emergence of blueschists on Earth linked to secular changes in oceanic crust composition: : Nature Geoscience, v. 9, no. 1, p. 60–64.10.1038/ngeo2605
Parkinson, I.J., and Pearce, J.A., 1998, Peridotites from the Izu–Bonin–Mariana forearc (ODP Leg 125): Evidence for mantle melting and melt–mantle interaction in a supra-subduction zone setting: Journal of Petrology, v. 39, no. 9, p. 1577–-1618.10.1093/petroj/39.9.1577
Paulick, H., Bach,W., Godard, M., De Hoog, J.C.M., Suhr, G., and Harvey, J., 2006, Geochemistry of abyssal peridotites (Mid- Atlantic ridge, 15°20′ N, ODP leg 209): Implications for fluid/rock interaction in slow spreading environments: Chemical geology, v. 234, p. 179–210. 10.1016/j.chemgeo.2006.04.011
Pearce, J.A., Barker, P.F., Edwards, S.J., Parkinson, I.J., and Leat, P.T., 2000, Geochemistry and tectonic significance of peridotites from the south sandwich arc-basin system South Atlantic: Contributions to Mineralogy and Petrology, v. 139, no. 1, p. v. 36–53 10.1007/s004100050572
Pearce, J.A., van der Laan, S.R., Arculus, R.J., Murton, B.J., Ishii, T., Peate, D.W., and Parkinson, I.J., 1992, Boninite and harzburgite from Leg 125 (Bonin-Mariana forearc): A case study of magma genesis during the initial stages of subduction, in proceedings of the ocean drilling program, scientific results, ocean drilling program: College Station, TX, v. 125, p. 623–659
Peighambari, S., Ahmadipour, H., Stosch, H.-G., and Daliran, D., 2011, Evidence for multi-stage mantle metasomatism at the Dehsheikh peridotite massif and chromite deposits of the Orzuieh coloured mélange belt, southeastern Iran: Ore Geology Reviews, v. 39, no. 4, p. 245–264.10.1016/j.oregeorev.2011.03.004
Pirnia, T., Arai, S., Tamura, A., Ishimaru, S., and Torabi, G., 2014, Sr enrichment in mantle pyroxenes as a result of plagioclase alteration in lherzolite: Lithos, v. 196-197, p. 198–212.10.1016/j.lithos.2014.03.008
Pirnia, T., Saccani, E., and Arai, S., 2018, Spinel and plagioclase peridotites of the Nain ophiolite (Central Iran): Evidence for the incipient stage of oceanic basin formation: Lithos, v. 310-311, p. 1–19.10.1016/j.lithos.2018.04.001
Rajabzadeh, M.A., Nazari Dehkordi, T., and Caran, S., 2013, Mineralogy, geochemistry and geotectonic significance of mantle peridotites with high-Cr chromitites in the Neyriz ophiolite from the outer Zagros ophiolite belts: Iran: Journal of African Earth Sciences, v. 78, p. 1–15
Reagan, M.K., Ishizuka, O., Stern, R.J., Kelley, K.A., Ohara, Y., Blichert-Toft, J., Bloomer, S.H., Cash, J., Fryer, P., Hanan, B.B., Hickey-Vargas, R., Ishii, T., Kimura, J.I., Peater, D.W., Rowe, M.C., and Woods, M. 2010, Fore-arc basalts and subduction initiation in the Izu–Bonin–Mariana system: Geochemistry, Geophysics, Geosystems, v. 11, no. Q03X12, 10.1029/2009GC002871
Sepidbar, F., Khedr, M.Z., Ghorbani, M.R., Palin, R.M., and Xiao, Y., 2021, Petrogenesis of arc-related peridotite hosted chromitite deposits in Sikhoran-Soghan mantle section, South Iran: Evidence for proto-forearc spreading to boninitic stages: Ore Geology Reviews, v. 136, p. 104256.10.1016/j.oregeorev.2021.104256
Sepidbar, F., Lucci, F., Biabangard, H., Khedr, M.Z., and Jiantang, P., 2020, Geochemistry and tectonic significance of the Fannuj-Maskutan SSZ-type ophiolite (Inner Makran, SE Iran): International Geology Reviews, v. 62, no. 16, p. 2077–2104.10.1080/00206814.2020.1753118
Shahabpour, J., 2005, Tectonic evolution of the orogenic belt in the region located between Kerman and Neyriz: Journal of Asian Earth Sciences, v. 24, no. 4, p. 405–417.10.1016/j.jseaes.2003.11.007

Shervais, J.W., 2001, Birth, death, and resurrection: The life cycle of suprasubduction zone ophiolites: Geochemistry, Geophysics, Geosystems (G3) 2 (Paper# 2000GC000080).

Shirdashtzadeh, N., Torabi, G., and Samadi, R., 2017, Petrography and mineral chemistry of metamorphosed mantle peridotites of nain ophiolite (Central Iran): Journal of economic geology: Persian with English abstract, 10.22067/econg.v9i1.40728

Sun, S.S., and McDonough, W.F., 1989, Chemical and isotopic systematics of oceanic basalt: Implications for mantle composition and processes. Saunders, A.D., and Norry, M.J. (), eds. Magmatism in the ocean basins: special publication, special publication, Vol. 42, no. p, p. 313–345

Takahashi, E., Uto, K., and Schilling, J.G., 1987, Primary magma compositions and Mg/Fe ratios of their mantle residues along Mid-Atlantic ridge 29N to 73N: Technical Rept, v. 9, p. 1–14.ISEI, Ser. A

Torabi, G., 2001, Causes of different composition of chromitites in Naein and Ashin ophiolites, and its absence in Anark and Jandaq ophiolites (Isfahan province: Petrology, v. 7, p. 1–20. Persian with English abstract.

Whattam, S.A., and Stern, R.J., 2011, The 'subduction initiation rule': A key for linking ophiolites, intra-oceanic forearcs, and subduction initiation: Contributions to Mineralogy and Petrology, v. 162, no. 5, p. 1031–1045.10.1007/s00410-011-0638-z

Workman, R.K., and Hart, S.R., 2005, Major and trace element composition of the depleted MORB mantle (DMM): Earth Planetary Science Letters, v. 231, no. 1–2, p. 53–72.10.1016/j.epsl.2004.12.005

Zaeimnia, F., Kananian, A., Arai, S., Mirmohammadi, M., Imamalipour, A., Khedr, M.Z., Miura, M., and Abbou-Kebir, K. 2017, Mineral chemistry and petrogenesis of chromitites from the Khoy ophiolite complex, north western Iran: Implications for aggregation of two ophiolites: Island Arc, v. 26, no. 6, p. e12211.10.1111/iar.12211

Zhou, M.F., Sun, M., Keays, R., and Kerrich, R., 1998, Control on platinum group elemental distributions of podiform chromitites: A case study of high Cr and high Al chromitites from Chinese orogenic belts: Geochimica et Cosmochimica Acta, v. 62, no. 4, p. 677–688.10.1016/S0016-7037(97)00382-7